Technical Report

TR-12-02

Buffer homogenisation, status report

Ann Dueck, Reza Goudarzi, Lennart Börgesson
Clay Technology AB

October 2011

Svensk Kärnbränslehantering AB
Swedish Nuclear Fuel
and Waste Management Co

Box 250, SE-101 24 Stockholm
Phone +46 8 459 84 00

ISSN 1404-0344
SKB TR-12-02

Buffer homogenisation, status report

Ann Dueck, Reza Goudarzi, Lennart Börgesson
Clay Technology AB

October 2011

Keywords: Bentonite, Swelling, Swelling pressure, Homogenisation.

Abstract

The present status report is a compilation of laboratory test results from tests done concerning homogenisation tests on a Wyoming bentonite. The main purpose of the status report is to provide results that can be used for modelling some well defined benchmark tests in order to improve the models or determine mechanical parameters for thermo-hydro-mechanical modelling of the behaviour of the buffer.

Results from fundamental laboratory tests and suggestions of future laboratory tests are presented. The data presented are preliminary and the report has not been through a factual and quality review.

Sammanfattning

Denna lägesrapport innehåller en sammanställning av laboratorieförsök som utförts för att studera homogeniseringsprocessen hos buffertmaterialet MX-80. Huvudsyftet med rapporten är att tillhandahålla resultat som kan användas för modellering av några väldefinierade prestandatester för att förbättra modellerna eller för att bestämma mekaniska parametrar för den termo-hydro-mekaniska modelleringen av buffertens uppförande.

Resultatet från grundläggande laboratorieförsök samt förslag för framtida försök presenteras.
De data som presenteras är preliminära och rapporten har inte genomgått sak- och kvalitetsgranskning.

Contents

1 Introduction

1.1 Background

Swelling of the buffer blocks and buffer homogenisation are important functions to guarantee the requirements of the buffer after full water saturation. It is important to understand and predict the final condition of the buffer after the swelling and homogenisation, which occurs both during the initial saturation and after a possible loss of bentonite caused by for example erosion.

Simplified material models have previously been used in the analyses of homogenisation processes. However, there are uncertainties in the models and the models need to be checked and improved, if necessary.

The project consists of four parts; theoretical studies, fundamental laboratory tests, laboratory study of the influence of friction and large scale tests of the scenario involving loss of bentonite. *The present status report describes the fundamental laboratory tests made so far, up to the end of 2010, in order to improve the knowledge of the involved processes and parameters.* Some planned studies of influence of friction and large scale tests are also briefly described.

1.2 Objective

The objective of the described tests has been to further improve the knowledge of the process of swelling and buffer homogenisation. The main purpose of the status report is to provide results that can be used for modelling some well defined benchmark tests in order to improve the models or determine mechanical parameters for thermo-hydro-mechanical modelling of the behaviour of the buffer.

2 Determination of basic variables

2.1 General

From each test the basic variables water content and bulk density are measured and from those variables the dry density and degree of saturation are calculated. During each test the radial and axial swelling pressures are measured.

2.2 Water content and bulk density determination

The basic geotechnical variables water content w (%), void ratio e, degree of saturation S_r (%) and dry density ρ_d (kg/m^3) are determined according to Equations 2-1 to 2-4.

$$w = 100 \cdot \frac{m_{tot} - m_s}{m_s} \tag{2-1}$$

$$e = \frac{\rho_s}{\rho}(1 + w/100) - 1 \tag{2-2}$$

$$S_r = \frac{\rho_s \cdot w}{\rho_w \cdot e} \tag{2-3}$$

$$\rho_d = \frac{m_s}{V} \tag{2-4}$$

where

m_{to} = total mass of the specimen (kg)

m_s = dry mass of the specimen (kg)

ρ_s = particle density (kg/m^3)

ρ_w = density of water (kg/m^3)

ρ = bulk density of the specimen (kg/m^3)

V = total volume of the specimen (m^3)

The dry mass of the specimen is obtained from drying the wet specimen at 105˚C for 24h. The bulk density is calculated from the total mass of the specimen and the volume is determined by weighing the specimen above and submerged into paraffin oil.

2.3 Swelling pressure determination

The swelling pressure is determined as axial and radial stresses exerted as loads on a piston with a certain area.

3 Material

The material used in the test series is the commercial Wyoming bentonite with brand name Volclay MX-80 from American Coll. Co. The powder is delivered with an approximate water content of 10%. Blocks made by compacted powder were used in the test series.

For determination of void ratio and degree of saturation the particle density ρ_s = 2,780 kg/m^3 and water density ρ_w = 1,000 kg/m^3 have been used.

4 Test technique

4.1 General

Swelling of water saturated bentonite specimens with access to water was studied in the following three test series, illustrated in Figure 4-1:

- Axial swelling in a device with constant radius and limited height. Variation of the height of the gap. (A0)
- Radial swelling of the outer surface in a device with constant height and limited radius. Variation of the radial gap. (R1)
- Radial swelling into a cylindrical cavity in a device with constant height and radius. Variation of the radius of the cavity. (R2)

The tests were mainly done with free swelling surfaces, i.e. no counteracting force until the swelling bentonite gel has reached the outer limited surface. In almost all tests the friction was minimized by use of a mineral-oil based lubricant on relevant surfaces.

4.2 Equipment

The three different types of test were carried out in devices with the design shown in Figure 4-2 to Figure 4-4.

The device used for the axial swelling consisted of a steel ring surrounding the specimen having filters on both sides. Two pistons were placed vertically, in the axial direction, above and below the specimen. A radial piston was placed in a hole through the steel ring for measurement of radial forces.

For both types of radial swelling a device was used which consisted of a steel ring surrounding the specimen having radial filters. A piston was placed vertically, in the axial direction, above the specimen. In this device a small horizontal radial piston was placed in a hole through the steel ring and through the radial filter for measurement of radial forces.

In both types of device the bottom and top plates and the steel ring were bolted together to keep the volume constant. Two load cells were placed in the vertical and radial direction, respectively. The load cells were placed between a fixed plate and the movable piston where the small deformation required by the load cell was admitted. During the entire course of the tests the forces were measured by the load cells which were calibrated prior to, and checked after, each test.

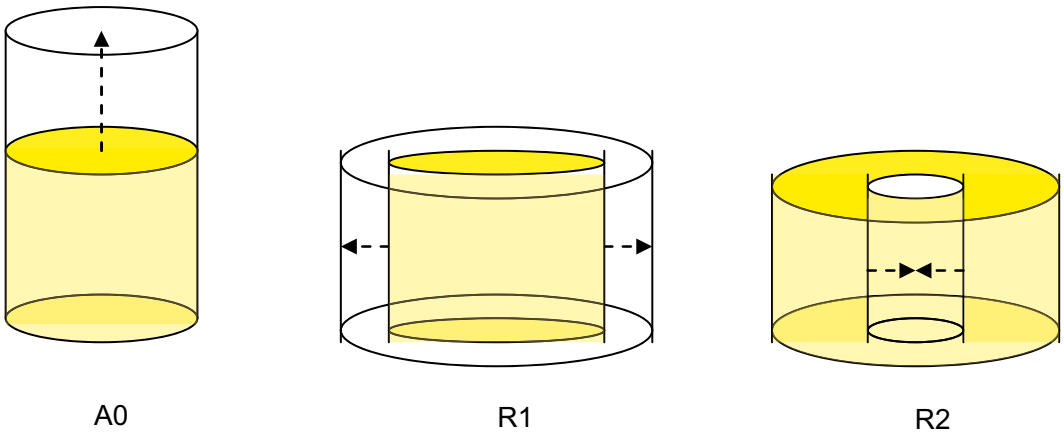

Figure 4-1. *Illustration of the geometry of the test types carried out.*

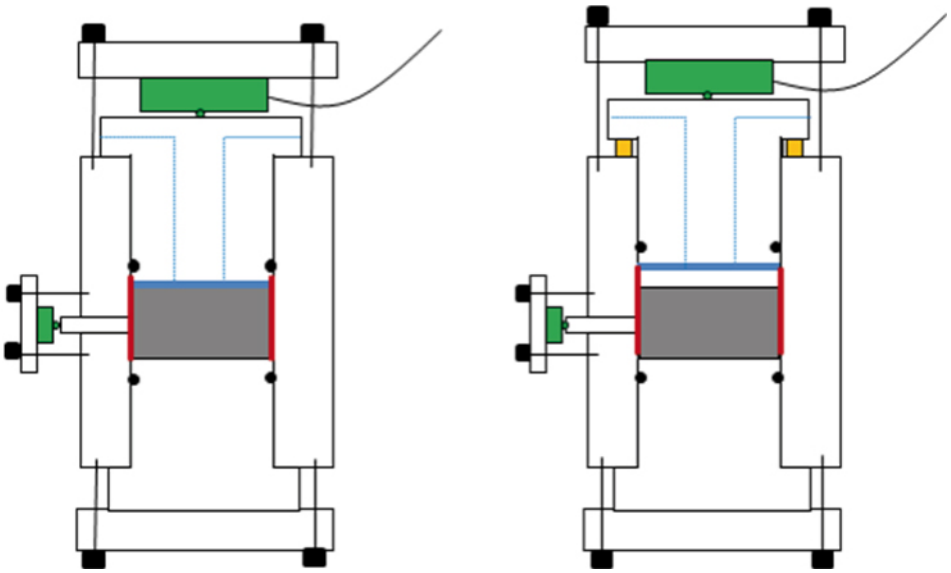

Figure 4-2. *Set-up used for the axial swelling tests (A). The red lines represent the lubricated surfaces and the blue lines represent filters and water supply.*

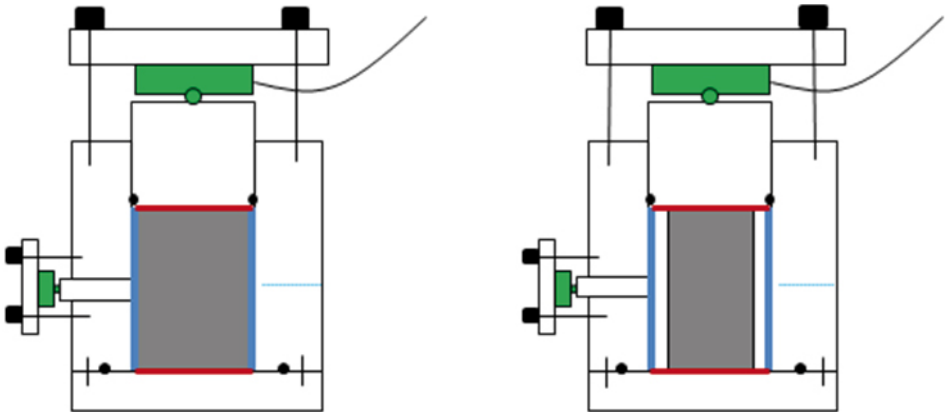

Figure 4-3. *Set-up used for the radial outward swelling tests (R1). The red lines represent the lubricated surfaces and the blue lines represent filters and water supply.*

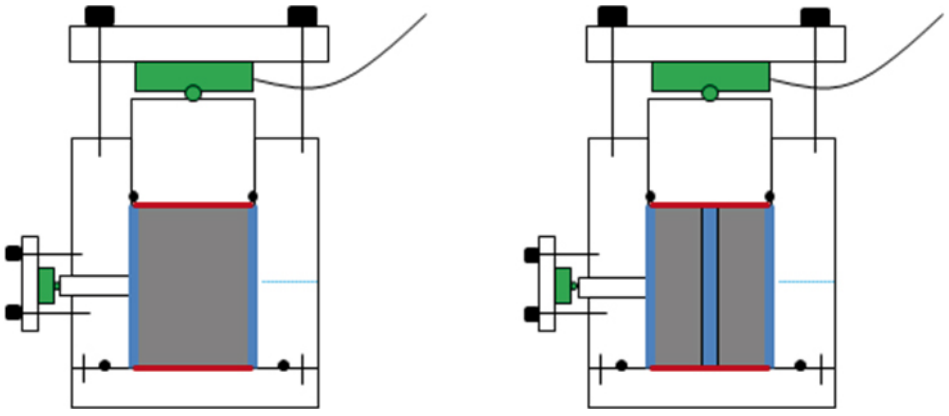

Figure 4-4. *Set-up used for the inward radial swelling tests (R2). The red lines represent the lubricated surfaces and the blue lines represent filters and water supply.*

4.3 Preparation of specimen

Cylindrical specimens were prepared by compaction of powder to a certain density. The specimens used for the axial type of swelling had a diameter of 50 mm and a height of 20 mm. For the radial types of swelling the diameter was 48 mm and the height 40 mm.

4.4 Test procedure

The tests consisted of two phases; the water saturation phase and the swelling phase. After mounting the specimen in one of the devices shown in Figure 4-2 to Figure 4-4, de-ionized water was applied to the filters after air evacuation of the filters and tubes. The specimens had free access to water during the water saturation. When only small changes in swelling pressure with time were noticed the water was evacuated from the filters and tubes and the second phase, i.e. the swelling, started. Depending on the type of swelling the following measures were taken;

- For the axial swelling (A0) the upper piston was moved upwards and fixed with spacers admitting a certain volume for the swelling. After evacuation of air, water was applied to the upper part of the specimen.
- For the radial swelling of the outer surface (R1) the water-saturated specimen was taken out and an outer volume was cut off the circumference of the specimen leaving a certain volume for swelling after re-mounting it in the same device. After evacuation of air the filter was filled with water.
- For the radial swelling of an inner cavity (R2) the lower lid was opened and a certain volume was drilled out from the center of the specimen. The cavity was filled with water, the lid was fixed and after evacuation of air the outer filter was filled with water.

After completed swelling and homogenisation, i.e. when no or negligibly small changes were noticed in the swelling pressure with time, the specimen was dismantled and cut in slices for determination of water content and density distribution in the direction of swelling.

4.5 Test results

The test results are presented with w, ρ_d and S_r as a function of the specimen height (series A0) or radius (series R1 and R2), i.e. as the distribution in the direction of swelling. The measured stresses are also shown and compared with a model of swelling pressure presented by Börgesson et al. (1995).

4.6 Test series

As described earlier three different types of swelling were studied; one type of axial swelling and two types of radial swelling. The axial swelling (A0) took place in the same direction as the compaction and the radial swelling (R1 and R2) took place perpendicular to the direction of compaction. However, two tests in series R1 were carried out on isostatically compacted specimens.

The proposed test series included swelling between 0 and 30% for each type of swelling (A0, R1 or R2). All specimens started with a dry density of approximately 1,656 kg/m^3 and after 30% of swelling the dry density was approximately 1,270 kg/m^3. The corresponding change in height and diameter for each test series are shown in Table 4-1. The swelling ratio is calculated as the change in volume divided by the initial volume.

Table 4-1. Final dimensions of the specimens used in each type of swelling. The range of change in height and diameter for each type of swelling is also given.

Test type	Swelling ΔV/V0 (%)	Final values of Height H (mm)	Diameter (mm)	Change in ΔH (mm)	circumferential ΔD1 (mm)	cavity ΔD2 (mm)
Axial A0	0–30	20–26	50	0–6		
Radial R1	0–30	40	46.8		0–6	
Radial R2	0–30	40	46.8			0– 1.2

5 Results

5.1 General

The results from each of the three series are presented separately in sections 5.2 to 5.4. Each presentation consists of diagrams with distribution of w, ρ_d and S_r in the direction of swelling. The presentation also contains diagrams of the axial and radial stresses, as a function of ρ_d, measured both after the initial water saturation at constant volume condition and after the subsequent steps of swelling. The stresses are compared with a model derived by Börgesson et al. (1995) (labeled TR-95-20 in the figures below). More details are presented in appendices where Appendix 1 contains diagrams of measured stresses as a function of time, Appendix 2 contains tables of the distribution of water content and density after termination and Appendix 3 contains a sum-up of the final values of water content, density, swelling pressure and the total time for each test.

The denomination of each specimen (the specimen ID) contains information about the test type, serial number and specimen number, e.g. A01-5 refers to specimen number 5 exposed to axial swelling, A0, in series 1. In the first part of the test series, the results from some specimens were considered as unusable due to different problems and are consequently omitted in the following presentation.

5.2 Axial swelling

The completed tests of axial swelling are shown in Table 5-1. In Figure 5-1 to Figure 5-3 the distribution of w, ρ_d and S_r measured after termination of each test are shown. So far, only the tests involving swelling of approximately 25% and 40% have been completed. The labels shown in the diagrams include the specimen ID and the swelling in %. The swelling ratio was calculated as the change in volume to the initial volume, $\Delta V/V_0$.

Water was added from the upper side only, both at the initial saturation and during the swelling in all tests except A01-1 and A01-2. In test A01-1 water was added from both sides during the saturation and in test A01-2 water was added from both sides during both the saturation and the swelling. In addition, specimen A01-1 was made without lubricated steel surfaces.

Three specimens diverge from the others in that one specimen was never allowed to swell (A01-7) and two specimens (A01-5 and A01-8) swelled directly after mounting, i.e. from the dry state. For the specimens A01-5 and A01-7 the final w, ρ_d and S_r are only given as averages and plotted at the radius zero in Figure 5-1 to Figure 5-3.

Table 5-1. Specimens used in the series A01.

	Initial w (%)	Constant Radius (mm)	Height at compaction (mm)	Height in steps (mm)	Swelling in steps (%)	Remarks
A01-1	11	25	20	20, 21, 25	0, 5, 25	No lubrication, water from 2 sides
A01-2	11	25	20	20, 21, 25	0, 6, 26	Water from 2 sides
A01-3	12	25	20	20, 21, 22, 23, 24, 25	0, 6, 11, 16, 21, 26	
A01-5	12	25	20	25	26	No initial sat.
A01-7	12	25	20	20	0	No swelling
A01-8	11	25	20	25	26	No initial sat.
A01-9	10	25	20	25	26	
A01-10	10	25	20	28	38	

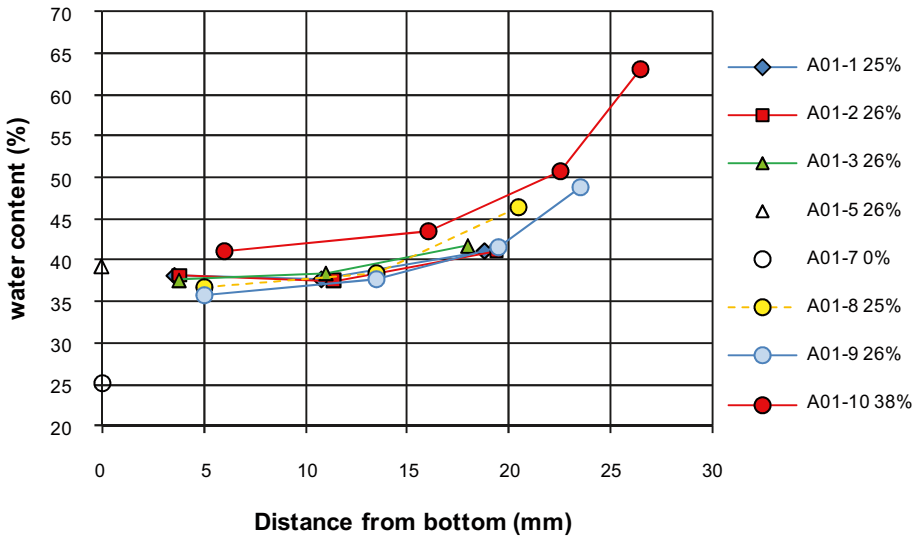

Figure 5-1. *Distribution of water content over the specimen height from series A01. The labels denote the type and number of specimen and the last figure denotes the swelling (%).*

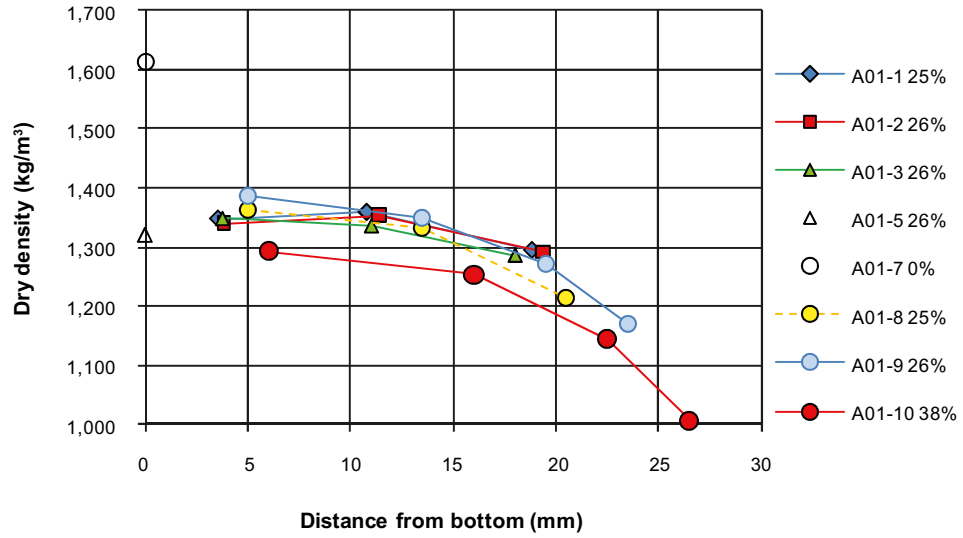

Figure 5-2. *Distribution of dry density over the specimen height from series A01.*

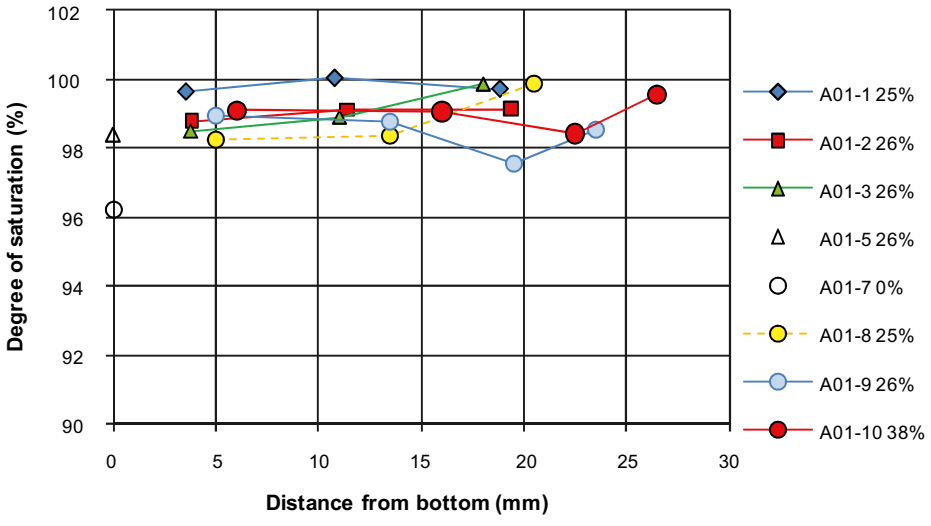

Figure 5-3. *Distribution of degree of saturation over the specimen height from series A01.*

The measured axial and radial stresses are shown in Figure 5-4 to Figure 5-7 as a function of dry density for all tests. The axial and radial stresses from each test were measured after the first saturation at constant volume condition and after the subsequent steps of swelling.

The average dry density after each step, used in Figure 5-4 to Figure 5-7, was calculated from the dry weight of the specimen and the volume inside the device at the different stage ($\rho_{d,calc}$). However, the final average dry density ($\rho_{d,meas}$) was also determined by calculating the average of the measured dry densities shown in Figure 5-2. The difference between the two types of dry densities according to Equation 5-1 was between –16 kg/m^3 and +22 kg/m^3. The error in the measured swelling pressure was for all tests less than 3%.

$$\Delta\rho_d = \rho_{d,calc} - \rho_{d,meas} \qquad (5\text{-}1)$$

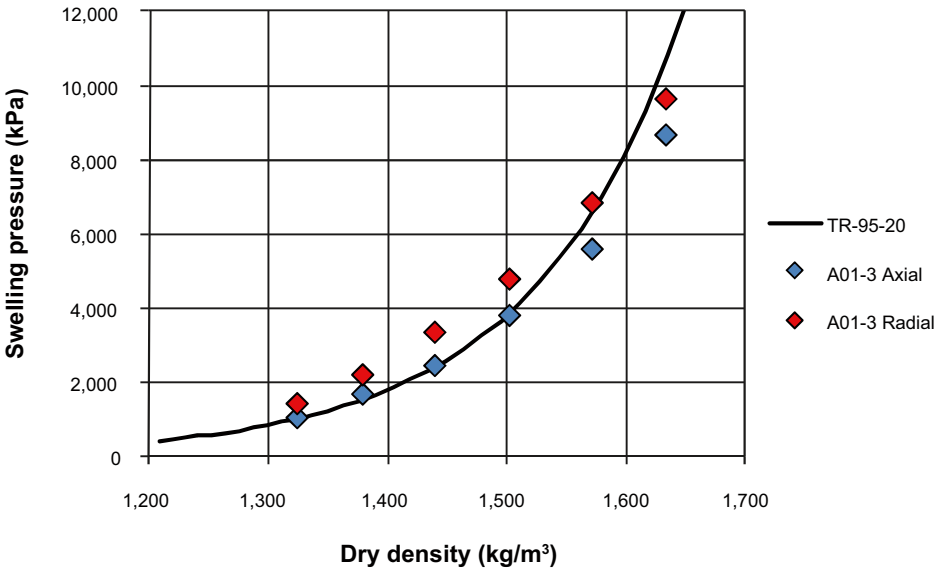

Figure 5-4. *Measured axial and radial stresses in test A01-3.*

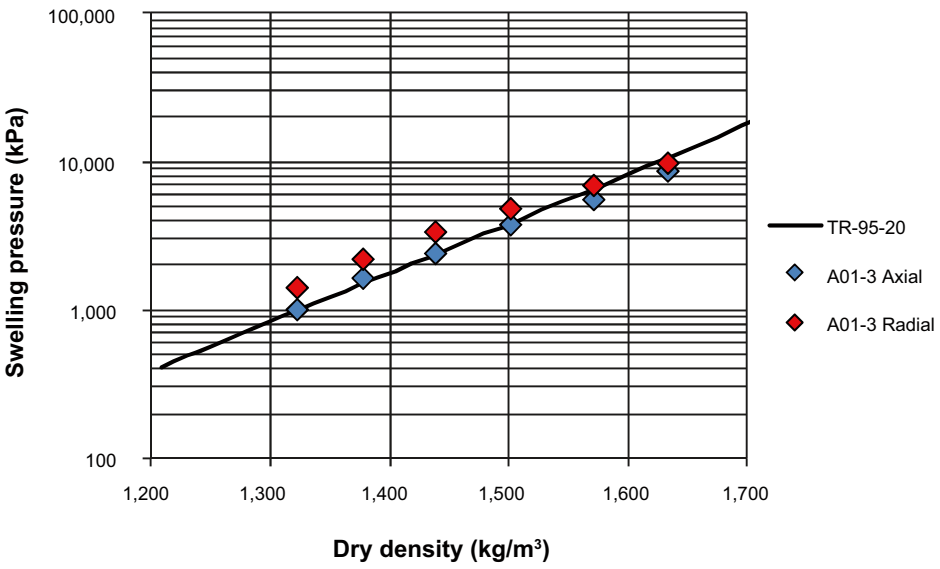

Figure 5-5. *Measured axial and radial stresses in test A01-3 (y-axis logarithmic).*

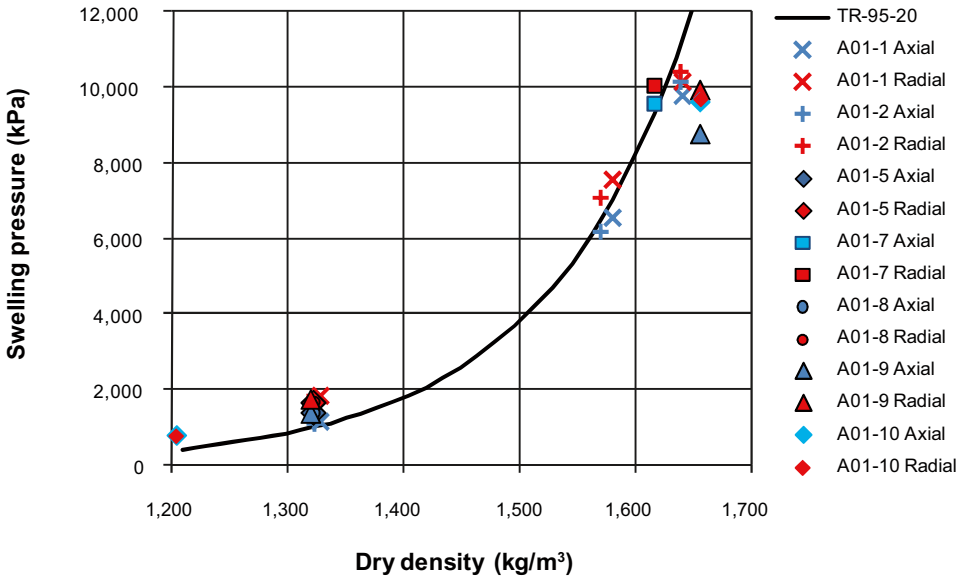

Figure 5-6. *Measured axial and radial stresses in tests A01-1, A01-2, A01-5, A01-7, A01-8, A01-9 and A01-10.*

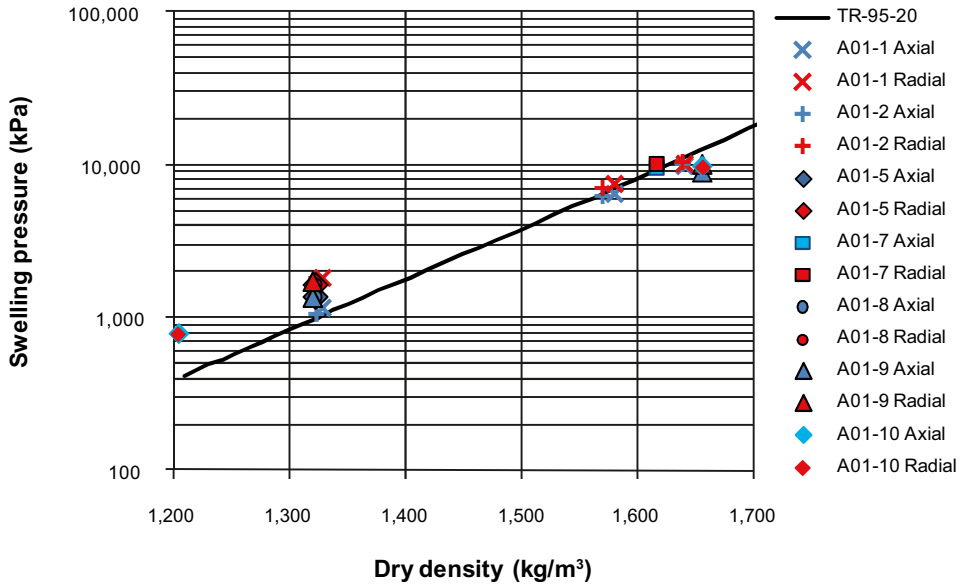

Figure 5-7. *Measured axial and radial stresses in tests A01-1, A01-2, A01-5, A01-7, A01-8, A01-9 and A01-10 (y-axis logarithmic).*

Observations

In general the main purpose of the report was to provide results that can be used for modelling, but the following observations could also be made:

- A high degree of saturation was achieved in all specimens after swelling.
- The distribution of w, ρ_d and S_r was similar in the six specimens subjected to 25–26% of axial swelling, irrespective of whether the swelling was made in one step from a more or less dry state or as a number of steps after an initial full saturation.
- A small deviation in the distribution of w and ρ_d was seen in the uppermost part of the results from the specimen starting from low degree of saturation (A01-8) compared to the other specimens exposed to the same amount of swelling, i.e. 25–26% swelling.

- After 25–26% swelling the distribution of w was not linear but increasing with increasing distance from the bottom end.
- The stresses correspond fairly well with the swelling pressure from the model presented by Börgesson et al. (1995).
- No significant deviation was seen from the results in the test that was run without lubricated surfaces.
- No large difference was seen between the average measured dry density $\rho_{d,meas}$ and the calculated $\rho_{d,calc}$.

5.3 Radial swelling of the outer surface

Radial outward swelling of the outer circumferential surface was studied in the tests shown in Table 5-2. In Figure 5-8 to Figure 5-10 the distributions of w, ρ_d and S_r determined after termination are shown. The labels shown in the diagrams include the specimen ID and the swelling in %. The colors blue, red, green and purple denote swelling of 3%, 5%, 14% and 31%, respectively. The swelling ratio was calculated as the change in volume to the initial volume, $\Delta V/V_0$.

The reduced diameter at the start of swelling D_{start} was calculated from the initial diameter D_0, the initial dry mass m_{s0} and the dry mass Δm_s cut off the specimen before the swelling, according to Equation 5-2.

$$D_{start} = \sqrt{\frac{m_{s0} - \Delta m_s}{m_{s0}}} \cdot D_0 \qquad (5\text{-}2)$$

Water was only added from the radial filter surrounding the specimen, both at the initial water saturation phase and at the subsequent swelling.

In addition to the proposed compacted specimens two samples were taken from an isostatically compressed larger block. There are, however, some uncertainties regarding the initial conditions of one of these specimens (R11-13).

Table 5-2. Specimens used in the series R11.

	Initial w (%)	Constant height (mm)	Initial diameter (mm)	Final diameter (mm)	Swelling $\Delta V/V_0$ (%)	Remarks
R11-1	12	40	46.8–3.0	46.8	14	Radial piston in contact with bentonite
R11-2	12	40	46.8–0.7	46.8	3	Radial piston in contact with bentonite
R11-5	12	40	46.8–1.1	46.8	5	Radial piston in contact with bentonite
R11-6	12	40	46.8–6.0	46.8	31	Radial piston in contact with bentonite
R11-7	12	40	46.8–3.0	46.8	14	
R11-9	10	40	46.8–6.0	46.8	32	
R11-10	10	40	46.8–0.7	46.8	3	
R11-11	10	40	46.8–1.1	46.8	5	
R11-12	10	40	46.8–1.1	46.8	5	Isostatic compaction
R11-13	10	40	46.8–6.0	46.8	30	Isostatic compaction
R11-14	10	40	46.8–3.0	46.8	14	
R11-15	20	40	46.8–3.0	46.8	14	
R11-16	21	40	46.8–3.0	46.8	16	Starting directly with swelling

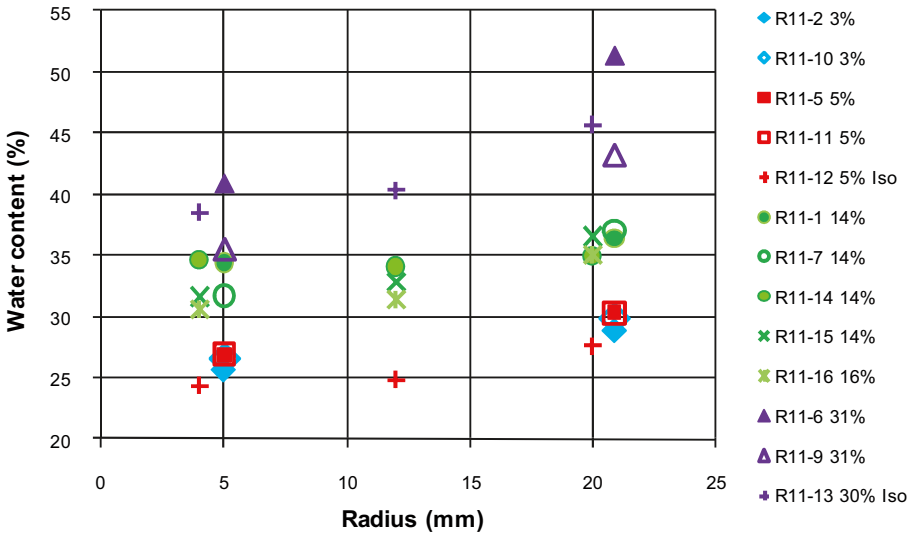

Figure 5-8. *Distribution of water content over the radius of the specimens from series R11. The labels denote the type and number of specimen and the last figure denotes the swelling (%).*

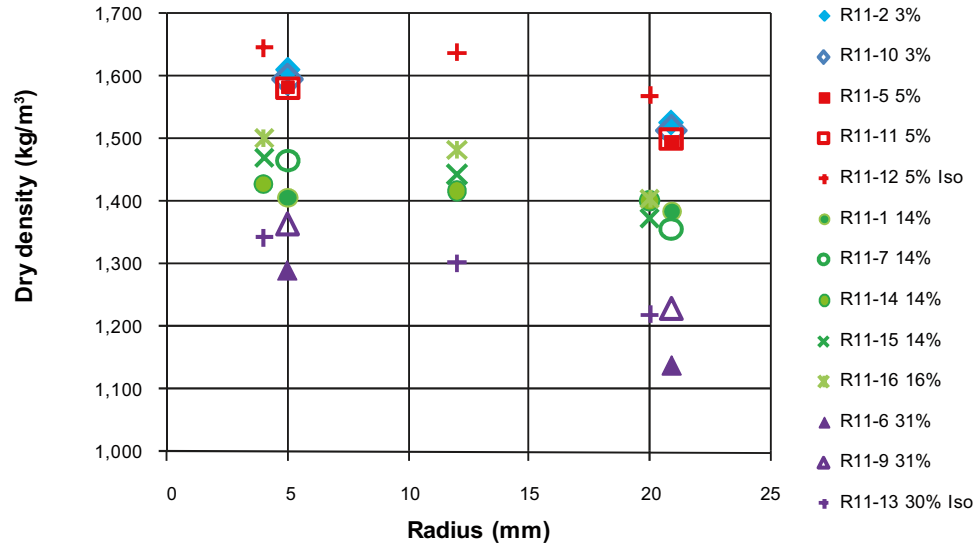

Figure 5-9. *Distribution of dry density over the radius of the specimens from series R11.*

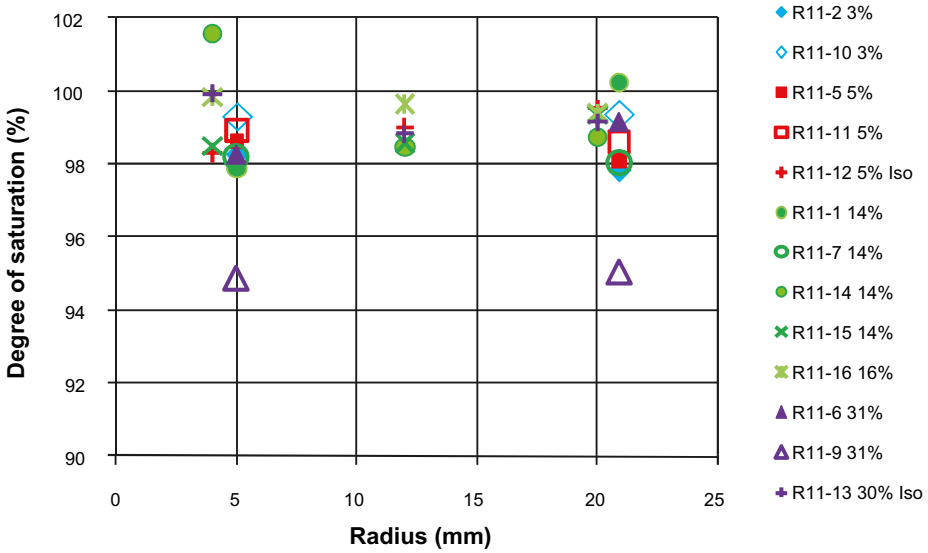

Figure 5-10. *Distribution of degree of saturation over the radius of the specimens from series R11.*

The degree of saturation was generally higher than 98%, with an exception of specimen R11-9. Specimen R11-9 swelled 31% and homogenised during about one week, a time period also used for other specimens in this series. However, a somewhat longer time period was used for the homogenisation of the other two specimens which swelled about 30%, R11-6 and R11-13. This longer time period might have been needed for the homogenisation in the case of large swelling

The stresses measured after the saturation phase and after the swelling in each test are shown in Figure 5-11 to Figure 5-14 as axial and radial stresses as a function of the average dry density. From each test two pairs of axial and radial stresses are shown which represent the stresses under constant volume condition and the stresses after subsequent swelling.

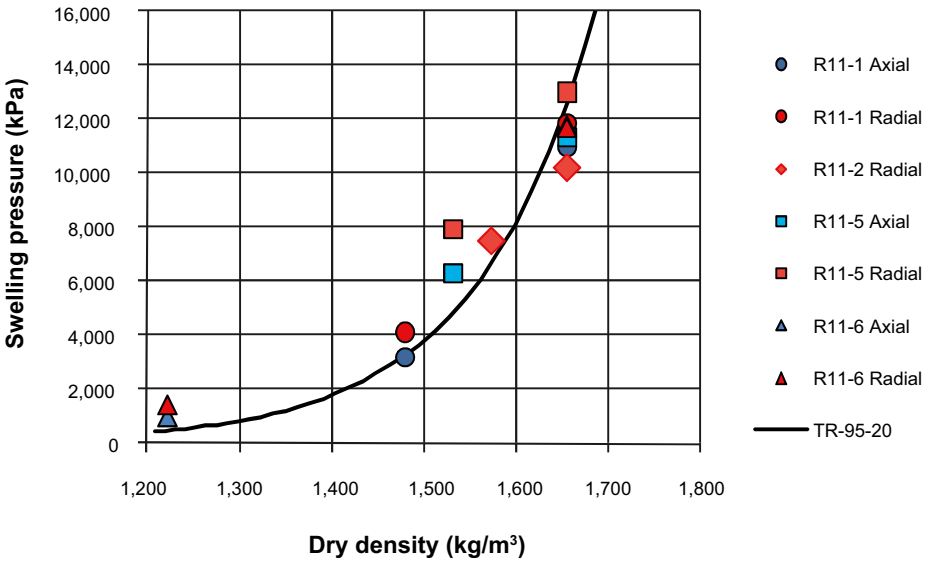

Figure 5-11. *Measured axial and radial stresses from tests R11-1, R11-2, R11-5 and R11-6. Only radial stresses from specimen R11-2. In these tests the radial piston was in contact with the specimen before swelling.*

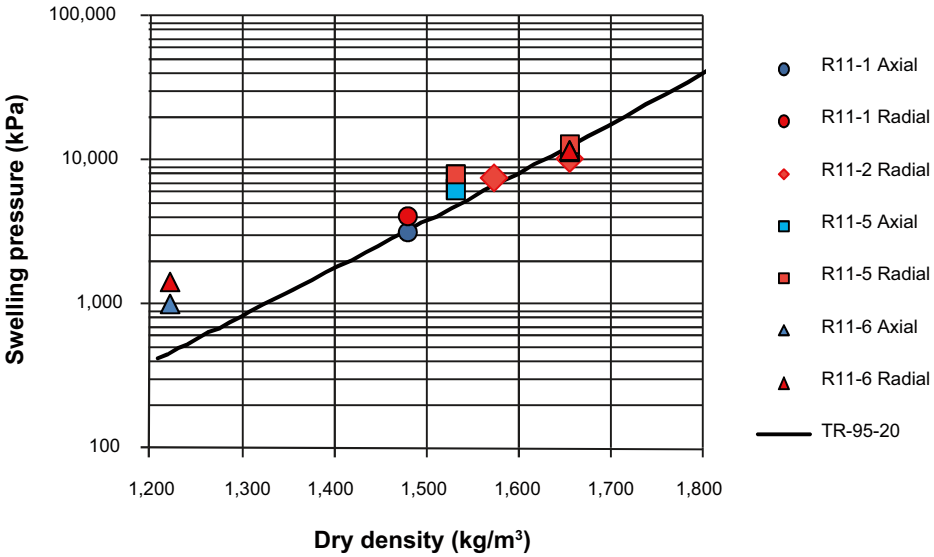

Figure 5-12. *Measured axial and radial stresses from tests R11-1, R11-2, R11-5 and R11-6.Only radial stresses from specimen R11-2. In these tests the radial piston was in contact with the specimen before swelling (y-axis logarithmic).*

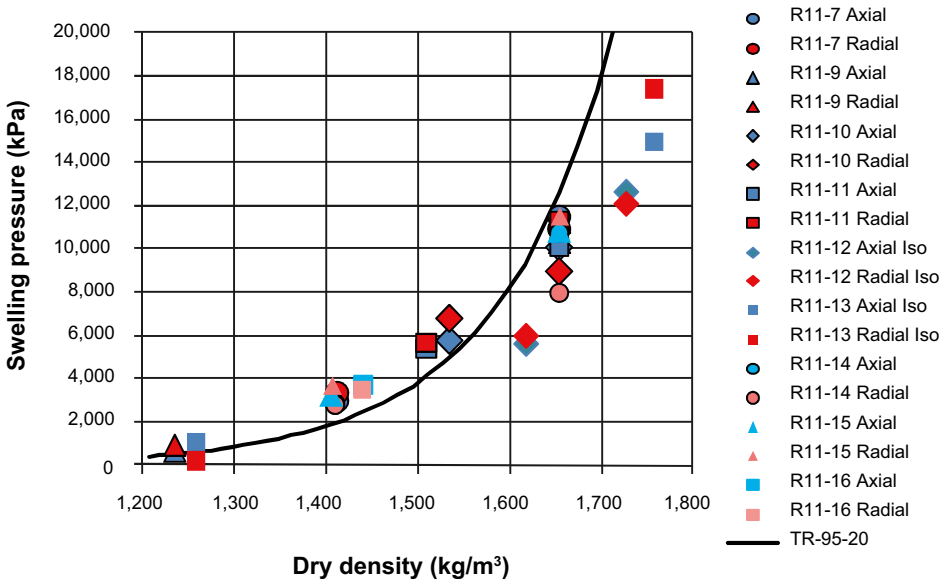

Figure 5-13. *Measured axial and radial stresses from tests R11-7, R11-9 and R11-10 to R11-16.*

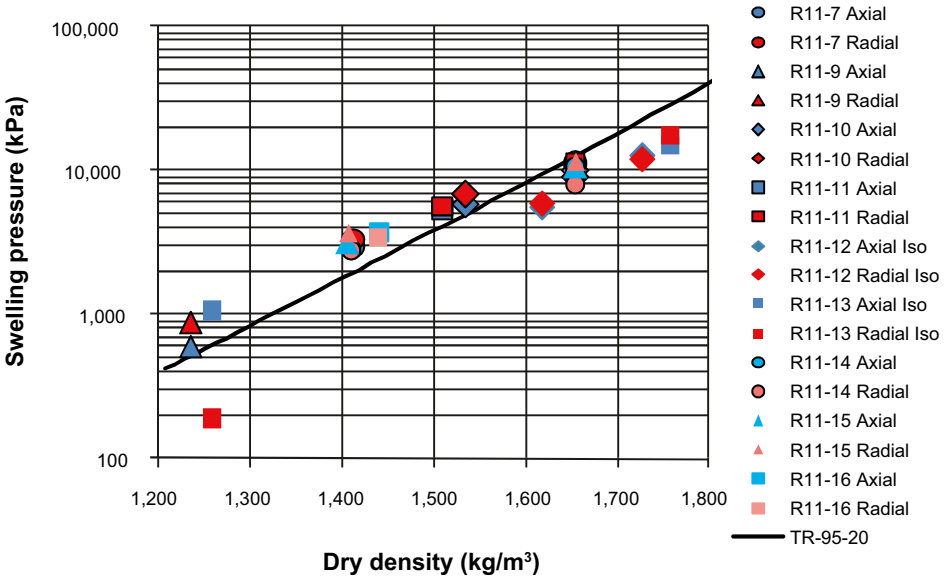

Figure 5-14. *Measured axial and radial stresses from tests R11-7, R11-9 and R11-10, R11-11 to R11-16 (y-axis logarithmic).*

During the test series it appeared that the measured radial stress was very sensitive to the initial location of the radial piston. Indications showed that different radial stresses were measured depending on whether or not the piston was in contact with the swelling bentonite before the final volume was reached. In tests R11-1 to R11-6 the radial piston was initially and deliberately put in contact with the bentonite when possible, while an attempt was made to initially avoid contact with the bentonite surface in the second part of the series, i.e. R11-7 to R11-16. However, it turned out that the air evacuation, before entering de-ionized water to the specimen, altered the initial position of the piston which gave that also in the second part of the series the piston could have been in contact with the bentonite before the final volume was reached. Thus, the presented radial stresses from tests R11-1 to R11-16 include some uncertainties.

After termination the average dry density was determined ($\rho_{d,meas}$) and this value was used in Figure 5-11 to Figure 5-14. The final dry density was also calculated ($\rho_{d,calc}$) according to Equation 5-3.

$$\rho_{d\,calc} = \frac{m_{s0} - \Delta m_s}{V} = \frac{m_{s0} - \frac{\Delta V}{V} m_{s0}}{V} \tag{5-3}$$

The difference between the calculated and the measured dry densities, Equation 5-1, was between –100 kg/m^3 and +70 kg/m^3 in this series. The majority of these values were positive which means that the dry density determined from measurements after termination was smaller than the one calculated from initial values, for almost all specimens. This could have been caused by swelling during dismantling. There is a tendency that the larger swelling during the test, the less difference between the calculated and measured dry densities after the test, according to Equation 5-1. This could follow from the stresses before the dismantling being less the larger swelling during the second phase of the tests. The error in the measured swelling pressure was less than 3%.

Observations

In general the main purpose of the report was to provide results that can be used for modelling, but the following observations could also be made:

- The gradients in w and ρ_d increased with the amount of swelling the specimens were exposed to.
- A high degree of saturation was achieved in all but one specimen after swelling. The low degree of saturation could have been caused by a too short time allowed for the homogenisation despite the swelling pressure being almost constant with time.
- No large difference is seen in the distribution of w and ρ_d between different test periods.
- All specimens swelled from full initial saturation except R11-16, which swelled from a degree of saturation of approximately 86%. No obvious influence of this difference could be seen.
- The stresses correspond fairly well with the swelling pressure from the model presented by Börgesson et al. (1995), especially after swelling.
- The dry density determined after termination was smaller for most of the specimens (9 of the performed 13 tests) compared to the calculated values based on the initial dry density. This could have been caused by swelling during dismantling. The difference decreased with increasing swelling during the second phase of the tests.
- The radial swelling pressure after swelling was higher than the axial in all tests except for two (R11-13 and R11-16). This is rather surprising and contradicts the results of tests series A01. However, some uncertainties were involved in the measured radial stresses in the present series.

5.4 Radial swelling into a cavity

Radial swelling into a cavity was studied in the tests shown in Table 5-3. The distributions of w, ρ_d and S_r determined after termination are shown in Figure 5-15 to Figure 5-17. The labels shown in the diagrams include the specimen ID and the swelling (%). The swelling ratio was calculated as the change in volume to the initial volume, $\Delta V/V_0$.

Water was added from the radial filter surrounding the specimen, both at the initial constant volume condition and at the subsequent swelling. In addition, the cavity was filled with water at start of the swelling.

Table 5-3. Specimens used in the series R21.

	Initial w (%)	Constant height (mm)	Outer diameter (mm)	Cavity diameter (mm)	Swelling $\Delta V/V_0$ (%)	Remarks
R21-3	12	40	46.8	8	3	
R21-5	12	40	46.8	10.5	5	
R21-6	12	40	46.8	19	20	
R21-7	12	40	46.8	–	0	
R21-8	12	40	46.8	23	32	

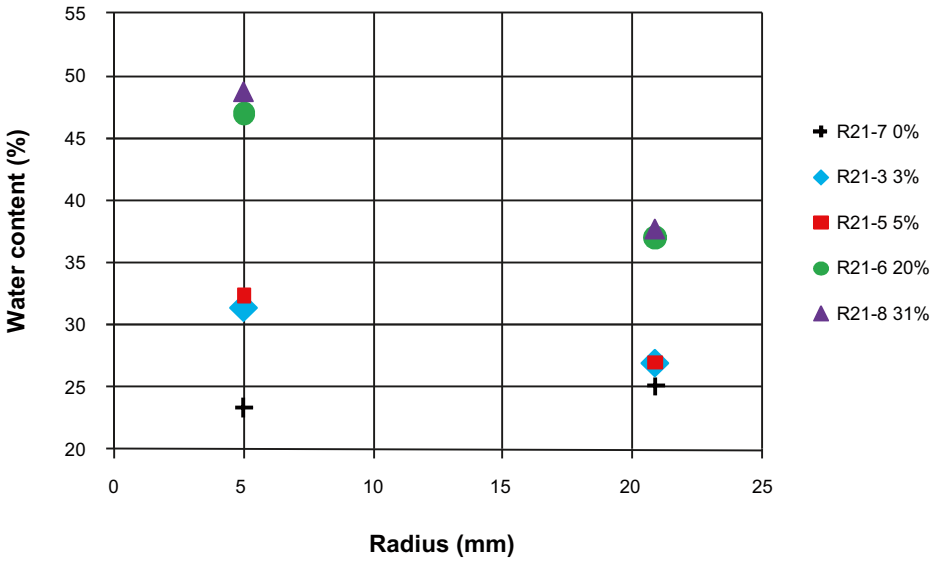

Figure 5-15. Distribution of water content over the radius of the specimens from series R21. The labels denote the type and number of the specimen and the last figure denotes the swelling (%).

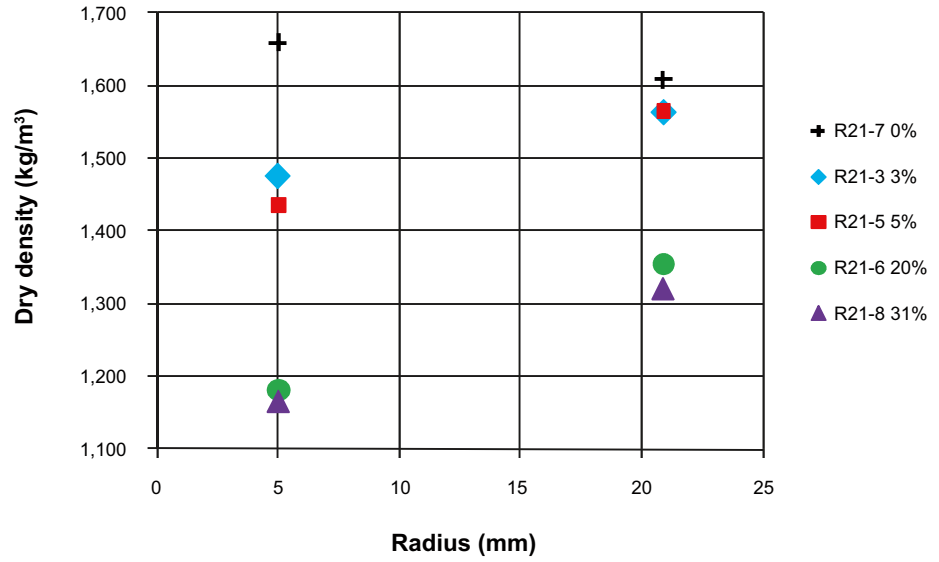

Figure 5-16. Distribution of dry density over the radius of the specimens from series R21.

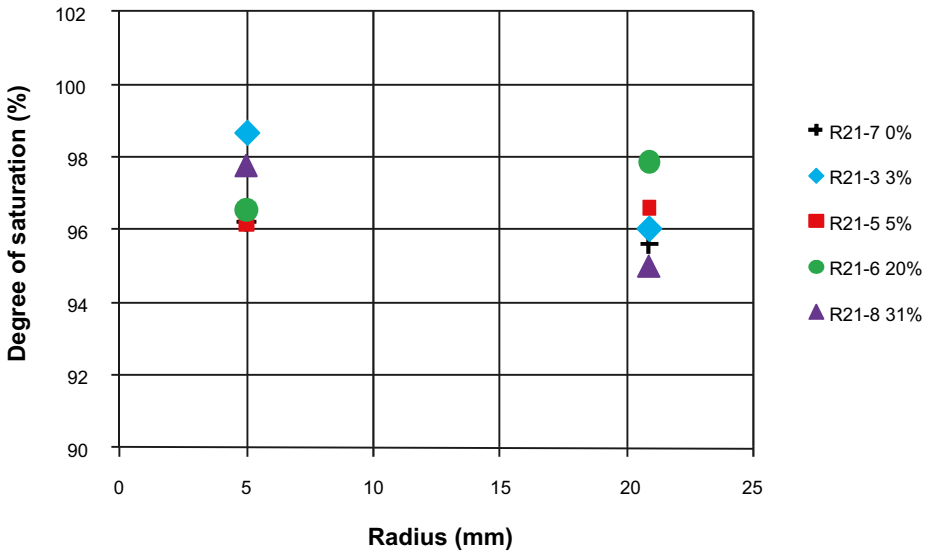

Figure 5-17. *Distribution of degree of saturation over the radius of the specimens from series R21.*

The degree of saturation was relatively low in the outer part of specimen R21-8, still after long time, while the inner part of the specimen could be considered as more or less saturated. This specimen swelled the most in this series and after dismantling a small cavity of about 4 mm in diameter was still seen on both sides of the specimen. This indicates that swelling still occurred and since the water initially filled into the cavity was limited it is likely that water was drawn from the outer part of the specimen where lower degree of saturation was also measured. Also specimen R21-7 suffered from relatively low degree of saturation which might be a consequence of relatively short time before dismantling was used for this specimen.

The measured stresses during each test are shown in Figure 5-18 and Figure 5-19 as axial and radial stresses as a function of dry density. The axial and radial stresses from each test were measured after completed water saturation at constant volume condition and after the subsequent swelling.

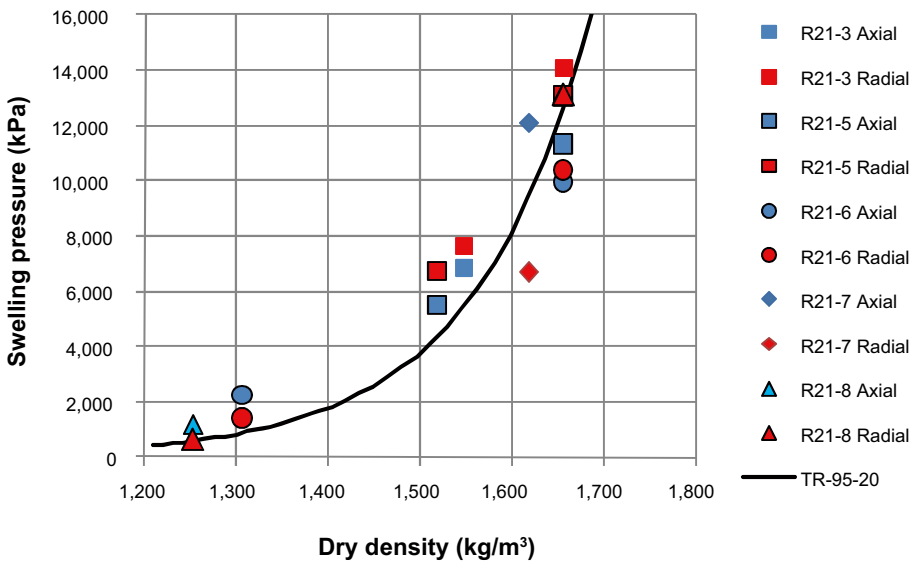

Figure 5-18. *Measured axial and radial stresses from all tests from series R21.*

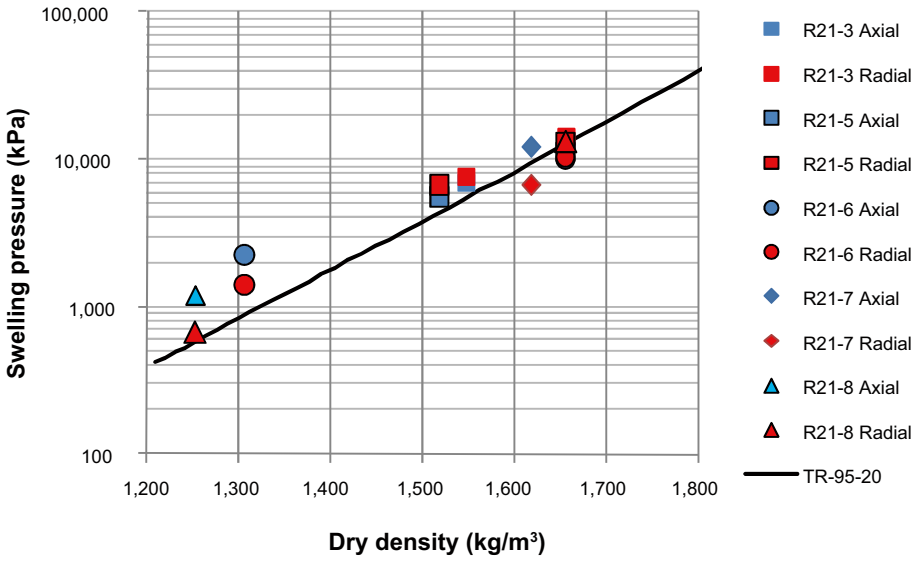

Figure 5-19. *Measured axial and radial stresses from all tests from series R21 (y-axis logarithmic).*

After termination the average dry density was determined, $\rho_{d,meas}$, and this value was used in Figure 5-18 and Figure 5-19. The final dry density was also calculated, $\rho_{d,calc}$, according to Equation 5-3.

The difference between the calculated and the measured dry densities, Equation 5-1, was between –122 kg/m^3 and +60 kg/m^3. The tendency is the same as for the specimens in series R1, indicating swelling during dismantling which decreased with decreasing final stresses before dismantling. The error in the measured swelling pressure was less than 3%.

Observations

In general the main purpose of the report was to provide results that can be used for modelling, but the following observations could also be made:

- A high degree of saturation was achieved in all specimens after swelling although the degree of saturation was lower than in the other series.
- The final gradients in w and ρ_d increased with the amount of swelling the specimens were exposed to.
- The stresses correspond fairly well with the swelling pressure from the model presented by Börgesson et al. (1995).
- Dry density determined after termination was smaller for almost all specimens compared to the calculated values based on the initial dry density. This could have been caused by swelling during the dismantling and it corresponds to the observations from series R1.
- The tests with large swelling (20% and 32%) yielded higher axial than radial stress, which is logical. However, the tests with little swelling (3% and 5%) yielded higher radial than axial stress. The latter is in agreement with series R1 but also difficult to explain.

5.5 Comments

In several of the tests with radial swelling, a larger radial stress than axial stress was measured, e.g. in R11-5, which was not expected. After completion of test series R1 it was concluded that the measurements of the radial stresses suffered from some uncertainties, cf. Section 5.3. However, the measuring technique used for the measurements of radial stresses was checked.

To check the measuring technique used for the measurement a test device was filled with water and water pressure was applied. The radial and axial stresses were measured according to the set-up shown in Figure 4-3 without the specimen. The determined stresses were found to correspond well with the applied water pressure. The maximum water pressure used was 2 MPa.

Another reason for too high radially measured stresses compared to axially measured stresses in the series involving radial swelling could have been presence of a large gradient in density in the perpendicular direction to the swelling, i.e. in the axial direction. The measurements could then be difficult to interpret.

To investigate the distribution of density in the axial direction two specimens were prepared to the same initial condition as the specimens used in the series with radial swelling i.e. series R1 and R2. One of the specimens was then saturated with the set-up shown in Figure 4-3. The resulting density distribution of the two specimens, representing before and after saturation, are shown in Figure 5-20.

The results in Figure 5-20 show a considerable density gradient before saturation while the density gradient after saturation and homogenisation is reduced but still exists. As in the case of the specimens used in series R1 and R2 a small swelling is involved in the first phase of the test, i.e. the initial saturation and homogenisation. In the radial swelling taking place in the second phase of these series the density gradient in the axial direction was expected to further decrease.

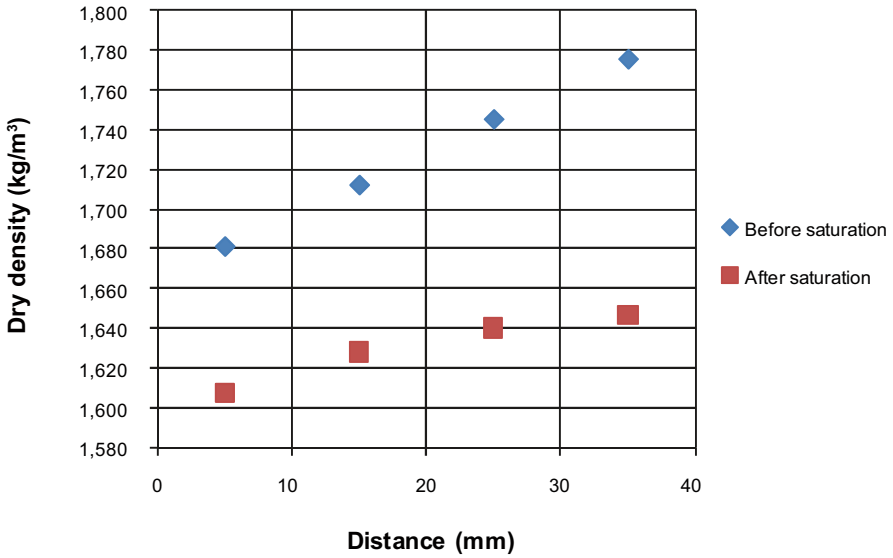

Figure 5-20. *Density distribution, before and after saturation, over the height of a specimen similar to those used in series R1 and R2.*

6 Plan for future homogenisation tests

6.1 General

New tests that are planned for in this project are briefly described below. Details of the tests and the number of tests to be run (given within brackets after each test type) are preliminary.

The coming test series consist of both basic tests of the same type as previously used where fundamental material parameters are studied, and of new test types where friction and self healing will be studied. With the previous test type the influence of initial conditions and material will be further studied. In a lager, but similar, device some of the completed tests will be repeated which will give larger resolution of the measured variables. New test types will be designed to study friction and self healing after loss of bentonite.

6.2 Basic tests of the same type as previously used

Completion of previous tests series

Some more tests with axial swelling (series A0) will be run where the swelling will deviate from 25%, which was previously used. Additional tests with radial swelling into a cavity (series R2) will also be done (4 tests).

Miscellaneous tests will be run to determine the distribution of water content and density more in detail, both after the saturation phase and after swelling, and to estimate the scatter in the results (4 tests).

Influence of initial conditions

The influence of some initial conditions needs to be further studied and the most important are the influence of

- direction of compaction,
- degree of saturation,
- initial inhomogeneous specimens.

There are question marks about the influence of the direction of compaction, so some of the tests made in previous series will be repeated on specimens sampled perpendicular to the direction of the compaction (3 tests).

The majority of the specimens in the previous test series swelled after completed saturation and only specimens A01-5, A01-8 and R11-16 started from a lower degree of saturation; 40%, 40% and 86%, respectively. The impact of a different initial degree of saturation at swelling will therefore be tested (3 tests).

The influence of initial homogeneity will be studied by use of specimens in two pieces having different properties. To begin with, differences in density will be tested. Two pieces with different densities will be put together to form one specimen which will be placed in the test equipment (3 test).

Influence of material

It is of interest to repeat some of the previous tests with another material preferably, a calcium dominated material in contrast to the sodium dominated MX-80 used so far (3–6 tests).

High resolution tests

A test series with larger dimensions is planned for in order to increase the resolution in the distributions of w and ρ after the test. The suggested device is shown in Figure 6-1. The saturation phase will be omitted in most tests in order to minimize the testing time and the specimen will therefore

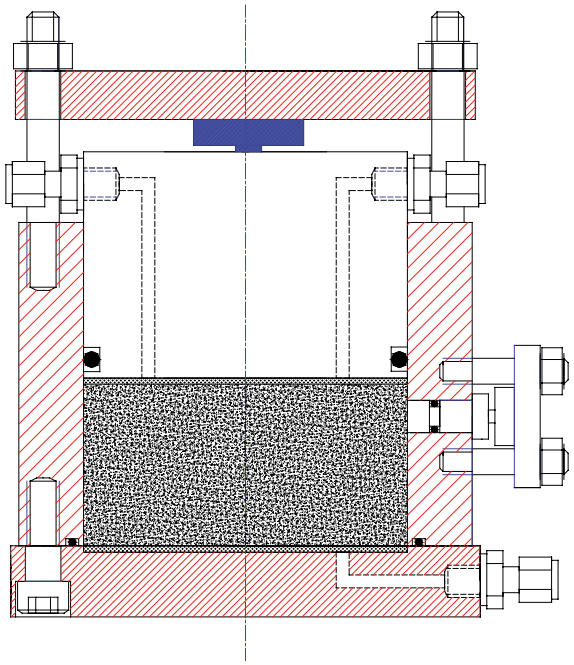

Figure 6-1. *Set-up proposed for the tests in larger scale.*

be prepared at high degree of saturation, i.e. at high water content. Radial plastic filters will be used. The time to equilibrium is estimated to be four times the required time for similar tests of the smaller size since these new specimens will have a diameter twice as big as the diameter of the previous specimen. Different densities will be used aiming at maximum swelling pressures of approximately 8 MPa.

6.3 Friction between buffer and other surfaces

Friction as applied stress

Friction between specimens at full swelling pressure and different types of surfaces will be studied with a new test device. The first part of the study includes the design of the equipment. A schematic view of the test type is shown in Figure 6-2 where the swelling pressure device with the specimen is placed in a frame. The ring of the device will then be pushed downwards while the force needed is measured.

In these tests the specimens will be saturated with a minimum of swelling and different densities will be used aiming at maximum swelling pressures of approximately 8 MPa. The tests can be made with and without lubricant on the surface of the ring surrounding the specimen.

Friction as reason for nonhomogeneous distribution of density

Friction will also be studied by introducing large density gradients over a specimen in a specially designed swelling pressure device. In this test type the effect of time will also be studied to further understand the homogenisation within a specimen even after the theoretically required time to get full pore pressure equalization. Several tests in equal tubes with for example 50 mm diameter and 300 mm height will be run at the same time. Enough time will be given for saturation and subsequent axial swelling and homogenisation. The specimens will be removed from the tubes after different time periods reaching up to several years so as to be able study the change in gradients of the base variables, i.e. w and ρ_d. (one series with approximately 4 tubes)

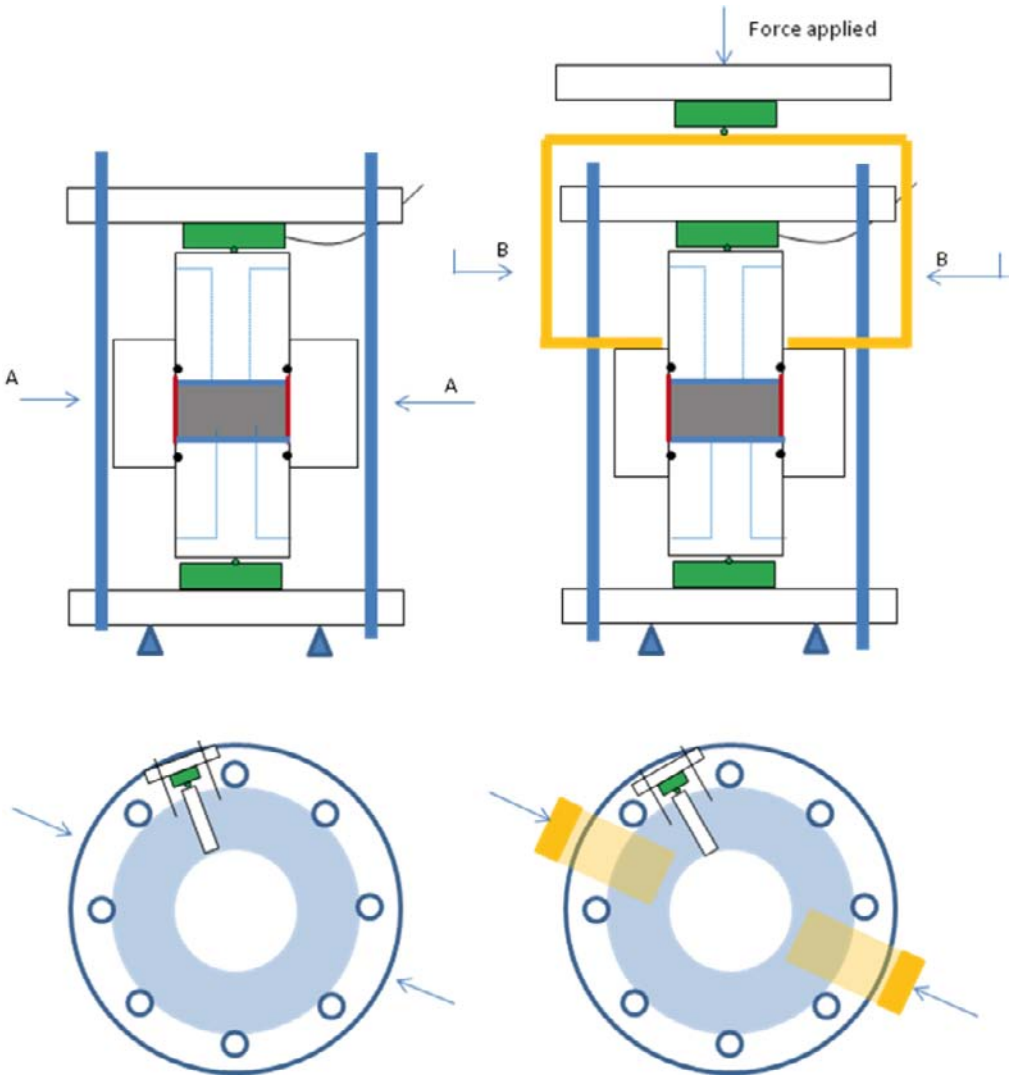

Figure 6-2. *Schematic outline of the test for the study of friction as applied stress.*

6.4 Self healing after loss of bentonite

Self healing of a larger cavity in a bentonite block will be investigated in a new test type. The test type was initiated by a theoretical study by Börgesson and Hernelind (2006). The objective is to have a cavity large enough to be able to a have good resolution of the sampling, but a small enough bentonite block to have a reasonable time to saturation. The set-up in Figure 6-3 is suggested, using a bentonite ring with a diameter of 300 mm and a height of 100 mm or larger, which is confined in both the outer and inner surfaces. The "heater" in Figure 6-3 will be optional.

In Figure 6-3 the initial condition is shown to the left and the suggested sampling after saturation is shown to the right with the lower part being a section of the upper. The sampling should be carefully planned to minimize evaporation and with the total of 1,215 marked samples it might be necessary to prioritize. The directions of the set-up can be changed to optimize the influence of gravity. (one test)

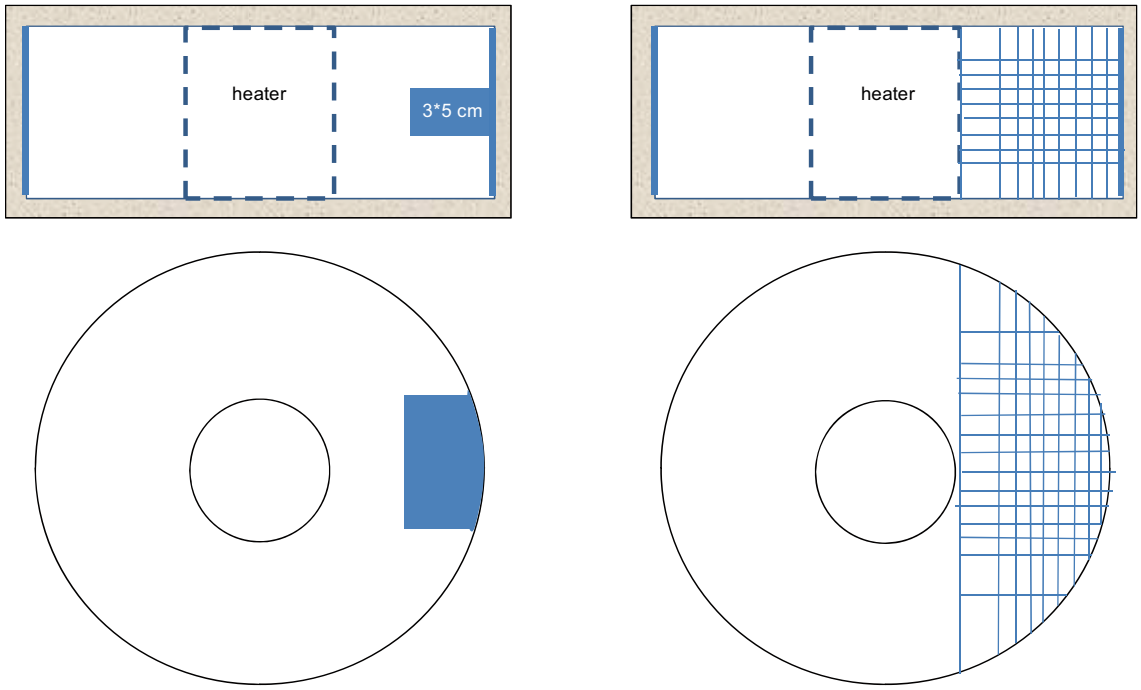

Figure 6-3. *Schematic set-up proposed for the self healing test.*

References

SKB's (Svensk Kärnbränslehantering AB) publications can be found at www.skb.se/publications.

Börgesson L, Hernelind J, 2006. Consequences of loss or missing bentonite in a deposition hole. A theoretical study. SKB TR-06-13, Svensk Kärnbränslehantering AB.

Börgesson L, Johannesson L-E, Sandén T, Hernelind J, 1995. Modelling of the physical behaviour of water saturated clay barriers. Laboratory tests, material models and finite element application. SKB TR 95-20, Svensk Kärnbränslehantering AB.

Swelling pressure development with time (diagrams)

Axial and radial swelling pressure development with time are given in diagrams for all tests. The evaluated height, void ratio and swelling for each step of each test are given in tables. Each series is presented in separate appendices.

A1-1 Axial swelling

A01-1 A01-1 Axial A01-1 Radial	**Test description:** Total of 3 steps; saturation and 2 steps of swelling (friction present) **Diameter of the specimen:** 50 mm							
	Height mm	Void ratio	*Axial stress* kPa	*Radial stress* kPa	Mean stress kPa	Accumulated swell (%) $\Delta H/H_0 = \Delta V/V_0$	Remarks	
	19.9	0.68	0	0			after comp.	
2008-10-24 00:00	20.1	0.68	423	814	684	0.8	start	
2008-11-18 11:00	20.2	0.69	9,748	10,141	10,010	1.4	saturation	
2008-11-18 11:25	20.9	0.76	1,168	3,118	2,468	5.0		
2008-12-12 14:35	20.9	0.76	6,513	7,553	7,206	5.2	swell 1	Measured
2008-12-12 14:36	24.9	1.09	59	3,487	2,344	25.1		e_{final}
2009-01-27 13:50	24.9	1.09	1,137	1,819	1,592	25.2	swell 2	1.09

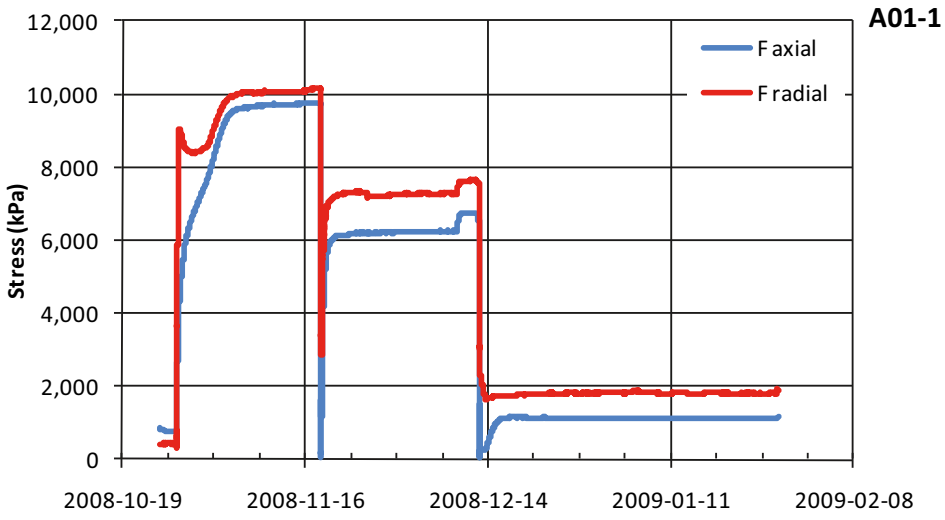

A01-2 A01-2 Axial A01-2 Radial	**Test description** Total of 3 steps; saturation and 2 steps of swelling (friction minimized) **Diameter of the specimen** 50 mm							
	Height mm	Void ratio	Axial stress kPa	Radial stress kPa	Mean stress kPa	Accumulated swell (%) $\Delta H/H_0 = \Delta V/V_0$	Remarks	
	19.9	0.68					after comp.	
2009-02-03 16:00	20.0	0.68	719	402	508	0.6	start	
2009-02-12 10:30	20.2	0.70	10,151	10,428	10,335	1.5	saturation	
2009-02-12 14:46	21.0	0.76	109	2,716	1,847	5.5		
2009-02-18 10:50	21.1	0.77	6,174	7,059	6,764	5.9	swell 1	Measured
2009-02-18 10:51	25.0	1.10	49	3,121	2,097	25.6		e_{final}
2009-03-02 00:00	25.0	1.10	1,065	1,826	1,572	25.7	swell 2	1.09

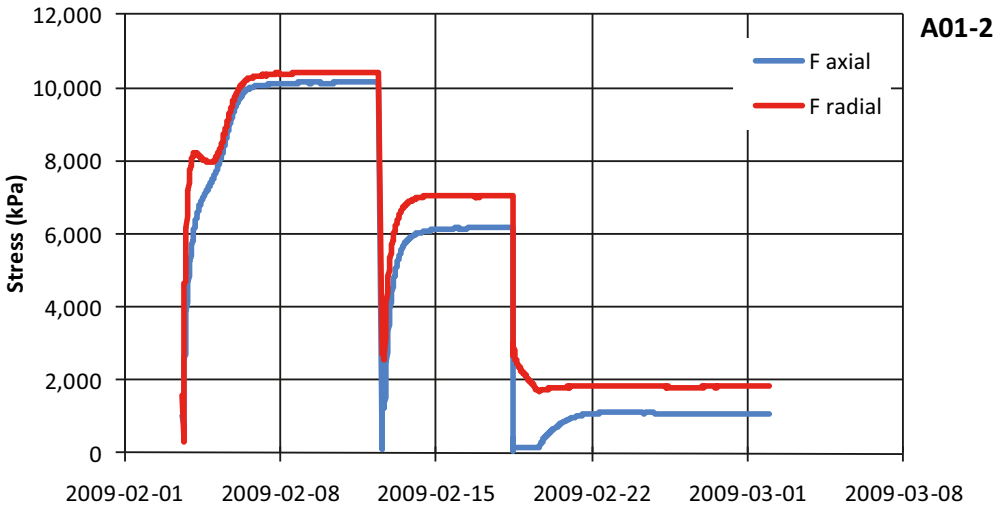

A01-3 A01-3 Axial A01-3 Radial	**Test description** Total of 6 steps; saturation and 5 steps of swelling (friction minimized) **Diameter of the specimen** 50 mm							
	Height mm	Void ratio	Axial stress kPa	Radial stress kPa	Mean stress kPa	Accumulated swell (%) $\Delta H/H_0 = \Delta V/V_0$	Remarks	
	19.91	0.68					after comp.	
2009-03-19 13:45	20.175	0.694	754	372	499	1.3	start	
2009-03-30 10:40	20.275	0.702	8,654	9,632	9,306	1.8	saturation	
2009-03-30 11:15	21.000	0.763	1,156	2,094	1,781	5.5		
2009-04-07 09:00	21.075	0.770	5,570	6,831	6,410	5.9	swell 1	
2009-04-07 09:40	22.000	0.847	977	2,493	1,988	10.5		
2009-04-15 15:47	22.050	0.851	3,777	4,773	4,441	10.7	swell 2	
2009-04-15 16:00	23.000	0.931	742	2,002	1,582	15.5		
2009-04-23 16:00	23.013	0.932	2,423	3,337	3,033	15.6	swell 3	
2009-04-23 16:20	24.000	1.015	457	1,679	1,272	20.5		
2009-05-04 08:30	24.025	1.017	1,653	2,191	2,012	20.7	swell 4	Measured
2009-05-04 09:10	25.000	1.099	241	1,118	826	25.6		e_{final}
2009-05-18 15:30	25.025	1.101	1,016	1,414	1,281	25.7	swell 5	1.10

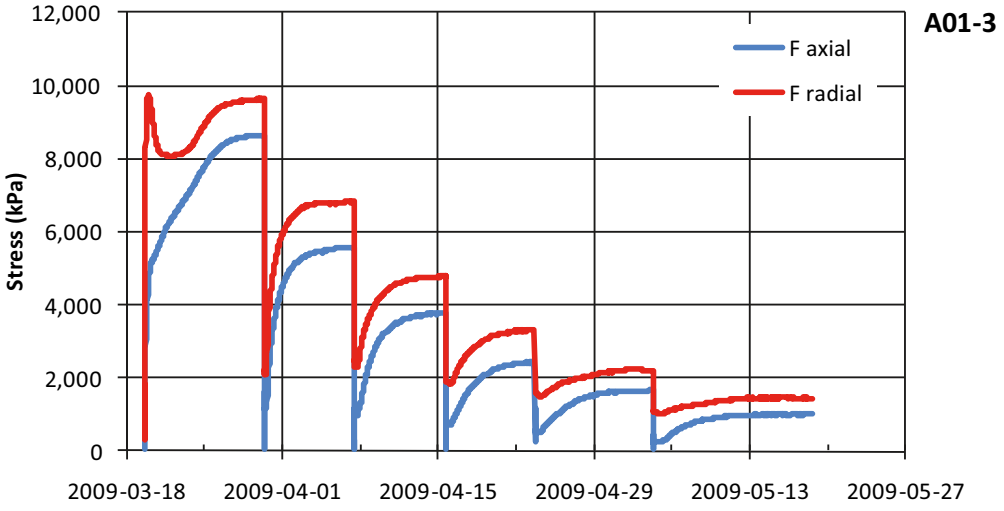

A01-5 A01-5 Axial A01-5 Radial	**Test description** Total of 1 step; lift and saturation (friction minimized) **Diameter of the specimen** 50 mm							
	Height mm	Void ratio	Axial stress kPa	Radial stress kPa	Mean stress kPa	Accumulated Remarks swell (%) $\Delta H/H_0 = \Delta V/V_0$		
	19.91	0.68					after comp.	Measured
2009-06-23 00:00	25.000	1.099	407	427	420	25.6	lift. start	e_{final}
2009-07-20 00:00	25.038	1.102	1,363	1,645	1,551	25.8	saturation	1.11

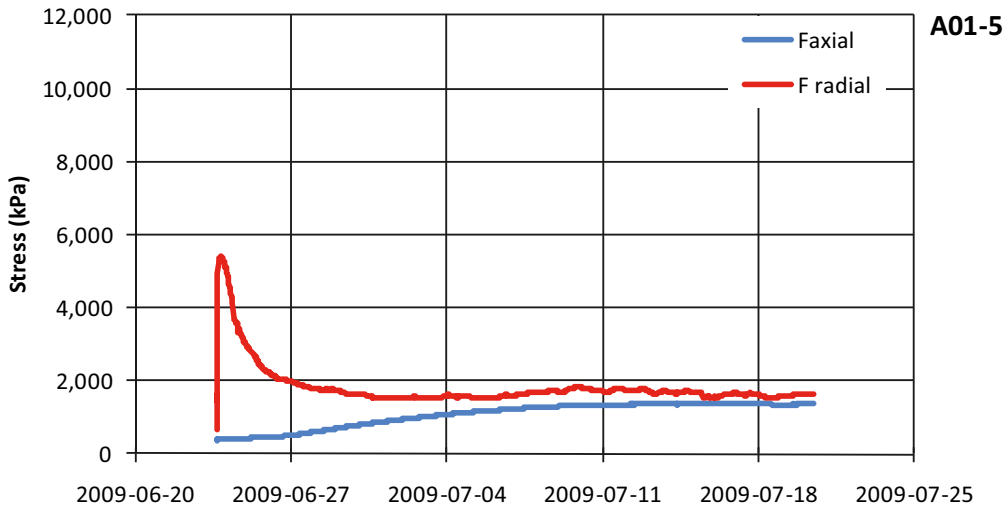

A01-7 A01-7 Axial A01-7 Radial	**Test description** Total of 1 step; only saturation (friction minimized) **Diameter of the specimen** 50 mm							
	Height mm	Void ratio	Axial stress kPa	Radial stress kPa	Mean stress kPa	Accumulated Remarks swell (%) $\Delta H/H_0 = \Delta V/V_0$		
	19.91	0.68	0	0			after comp.	Measured
2009-08-06 10:00	20	0.72	4,388	1,011	2,136		start	e_{final}
2009-08-18 10:30	20	0.72	9,548	10,045	9,879	0	saturated	0.72

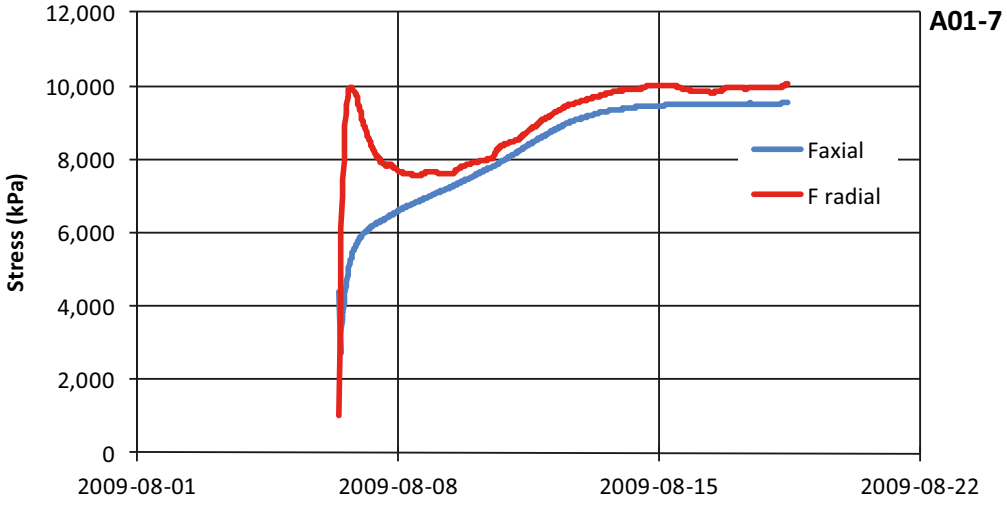

A01-8	Test description	Total of 1 step; lift and saturation (friction minimized)						
A01-8 Axial	Diameter of the specimen		50 mm					
A01-8 Radial	Height mm	Void ratio	Axial stress kPa	Radial stress kPa	Mean stress kPa	Accumulated swell (%) $\Delta H/H_0 = \Delta V/V_0$	Remarks	
	19.91	0.68					after comp.	Measured
2009-11-23 09:00	25.000	1.099	407	427	420	25.6	lift. start	e_{final}
2009-12-16 00:00	25.025	1.101	1,363	1,645	1,551	25.7	saturation	1.14

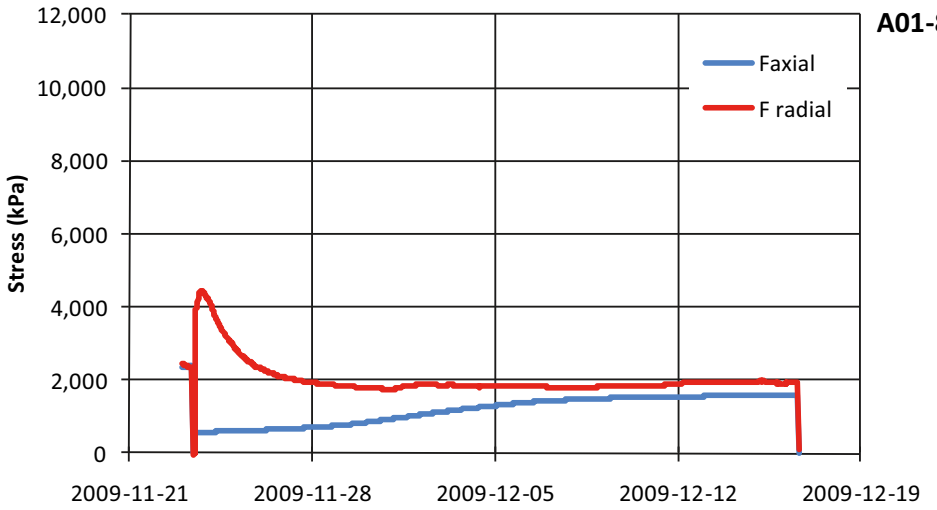

A01-9	Test description	Total of 2 step; saturation and 1 step of sw elling (friction minimized)						
A01-9 Axial	Diameter of the specimen		50 mm					
A01-9 Radial	Height mm	Void ratio	Axial stress kPa	Radial stress kPa	Mean stress kPa	Accumulated swell (%) $\Delta H/H_0 = \Delta V/V_0$	Remarks	
	19.9	0.68					after compaction	
2010-03-10 16:45	20.0	0.68	584	325	411	0.5	start	
2010-03-26 13:55	20.0	0.68	8,783	9,915	9,537	0.5	saturation	Measured
2010-03-26 14:06	25.0	1.10	1,100	2,102	1,768	25.6		efinal
2010-04-06 16:30	25.1	1.11	1,333	1,716	1,588	26.1	swell 1	1.10

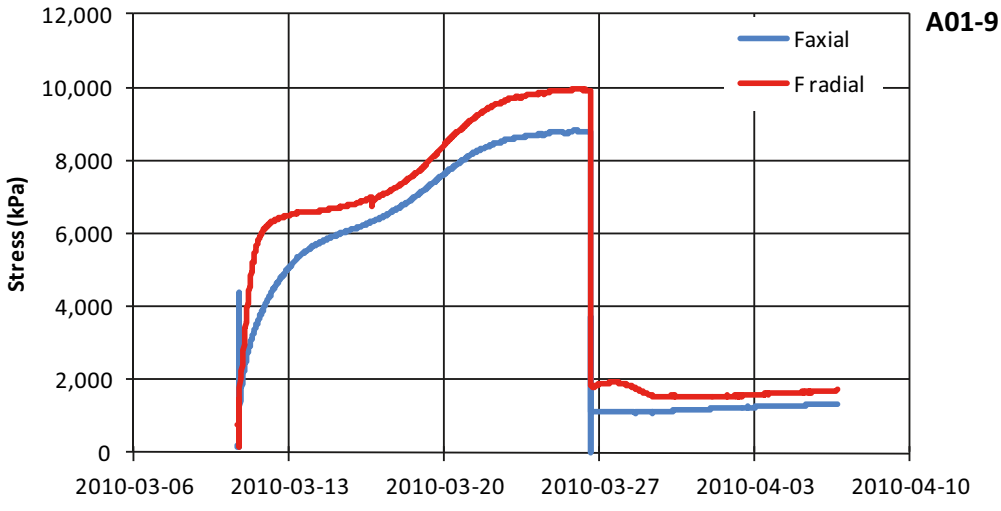

A01-10	**Test description**	Total of 2 step; saturation and 1 step of swelling (friction minimized)						
A01-10 Axial	**Diameter of the specimen**			50 mm				
A01-10 Radial	Height mm	Void ratio	Axial stress kPa	Radial stress kPa	Mean stress kPa	Accumulated swell (%) $\Delta H/H_0 = \Delta V/V_0$	Remarks	
	19.9	0.68					after compaction	
2010-04-08 11:27	20.0	0.68	617	191	333	0.5	start	
2010-04-26 08:00	20.0	0.68	9,631	9,698	9,675	0.5	saturation	Measured
2010-04-26 09:38	27.5	1.31	589	1,591	1,257	38.1		efinal
2010-05-18 13:00	27.5	1.31	771	775	774	38.1	swell 1	1.29

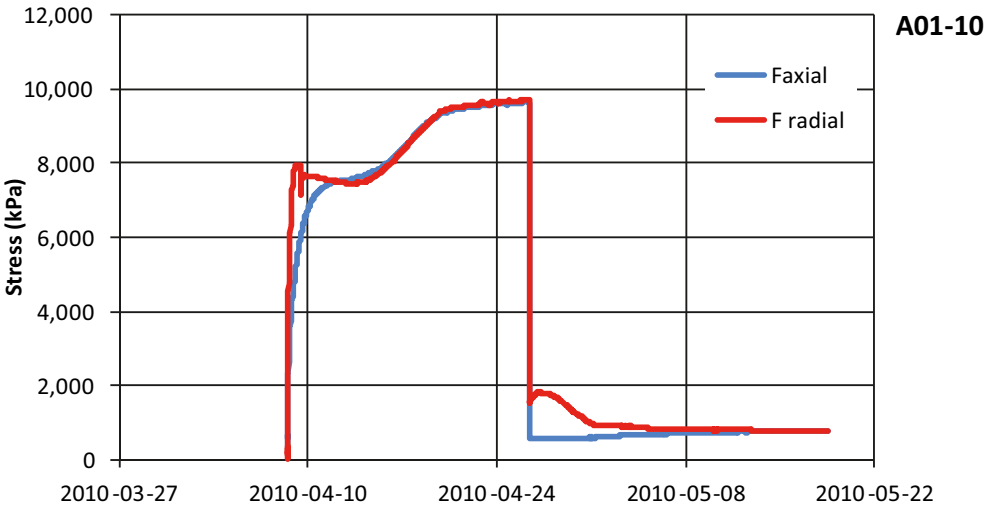

A1-2 Radial swelling of the outer surface

R11-1	Test description:	Total of 2 steps; saturation and 1 steps of swelling (friction minimized)						
R11-1 Axial	Constant height of specimen (mm)	40	Final diameter of specimen (mm)	46.8				
R11-1 Radial	Decrease in diameter mm	Void ratio	*Axial stress* kPa	*Radial stress* kPa	Mean stress kPa	Accumulated swell (%) $\Delta A/A_0 = \Delta V/V_0$	Remarks	Constants $m_{s.start}$ (g) 114
		0.62	0	0			after comp.	ρ_s (kg/m^3)
2009-04-08 17:15	0.0		916	735	795		start	2780
2009-04-16 13:30	0.0	0.68	10,965	11,871	11,569		saturation	e_{calc}
2009-04-16 15:33	3.0		913	1,509	1,310			
2009-04-22 12:35	0.0	0.88	3,162	4,111	3,795	14.2	swell 1	0.95

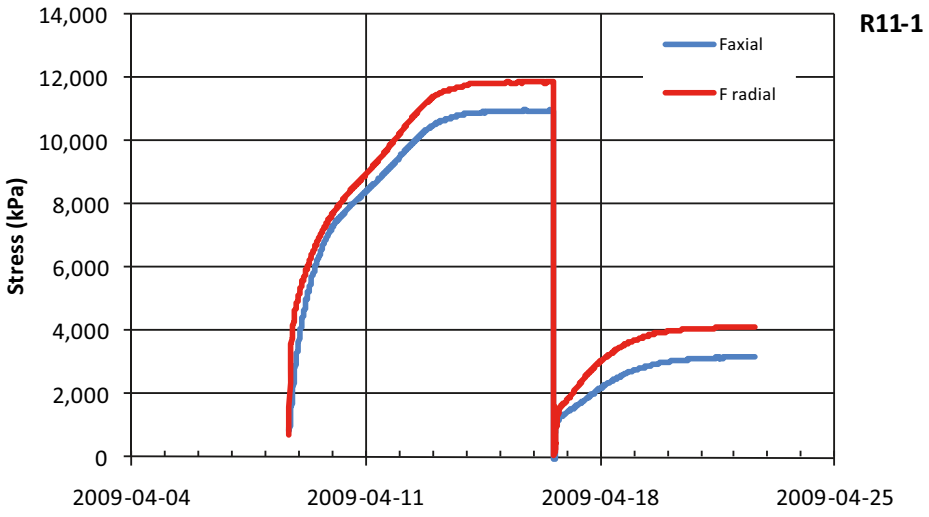

R11-2	Test description:	Total of 2 steps; saturation and 1 steps of swelling (friction minimized)							
R11-2 Axial	Constant height of specimen (mm)		40	Final diameter of specimen (mm)				46.8	
R11-2 Radial	Decrease in diameter mm	Void ratio	*Axial stress* kPa	*Radial stress* kPa	Mean stress kPa	Accumulated swell (%) $\Delta A/A_0 = \Delta V/V_0$	Remarks	Constants $m_{s.start}$ (g) 114	
		0.62		0			after comp.	ρ_s (kg/m^3)	
2009-05-04 17:22	0.0			1,026			start	2780	
2009-05-12 10:00	0.0	0.68		10,233			saturation	e_{calc}	
2009-05-12 11:46	0.7			569					
2009-05-27 13:30	0.0	0.77		7,530		3.0	swell 1	0.73	

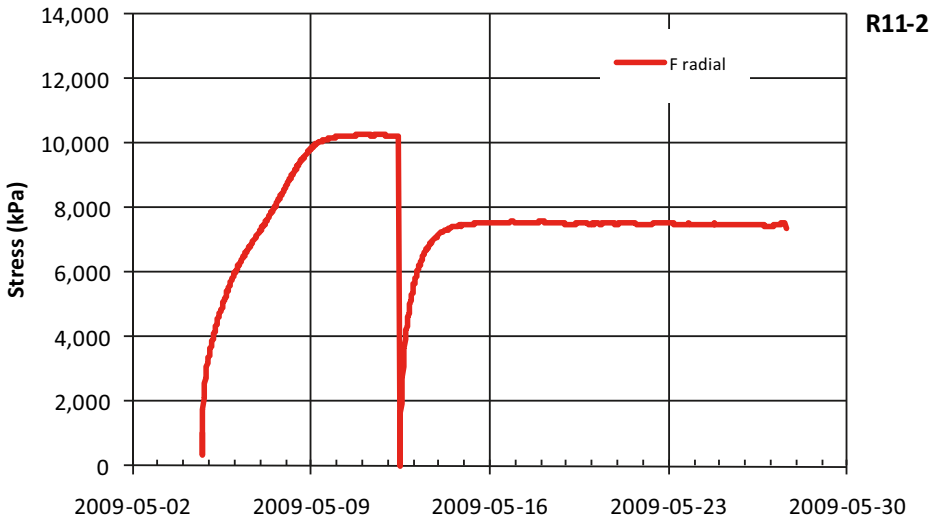

R11-5	Test description:	Total of 2 steps; saturation and 1 steps of swelling (friction minimized)						
R11-5 Axial	Constant height of specimen (mm)		40	Final diameter of specimen (mm)				46.8
R11-5 Radial	Decrease in diameter mm	Void ratio	*Axial stress* kPa	*Radial stress* kPa	Mean stress kPa	Accumulated swell (%) $\Delta A/A_0 = \Delta V/V_0$	Remarks	Constants $m_{s.start}$ (g) 114
		0.62	0	0			after comp.	ρ_s (kg/m^3)
2009-09-07 14:06	0.0		934	676	762		start	2780
2009-09-16 13:00	0.0	0.68	11,319	13,004	12,442		saturation	e_{calc}
2009-09-16 14:50	1.1		930	608	715			
2009-09-22 09:00	0.0	0.82	6,279	7,936	7,383	5.1	swell 1	0.77

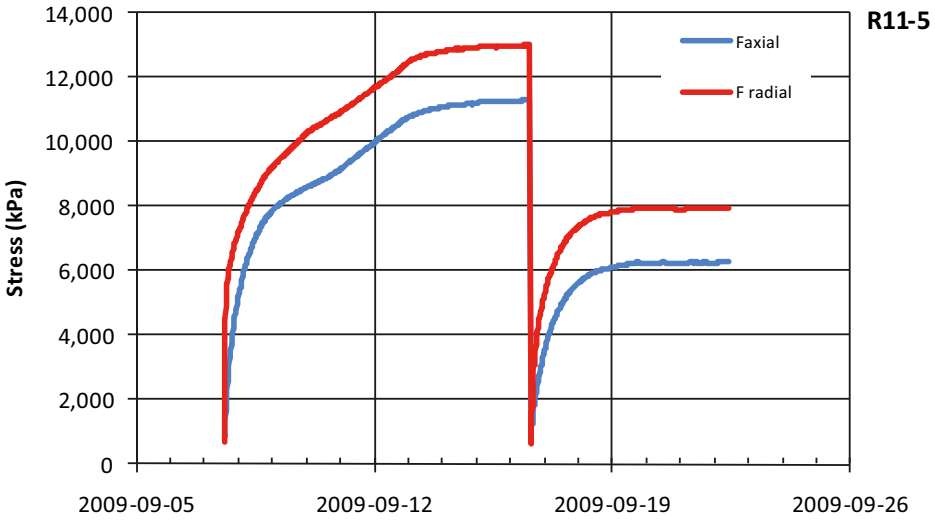

R11-6	Test description:	Total of 2 steps; saturation and 1 steps of swelling (friction minimized)						
R11-6 Axial	Constant height of specimen (mm)		40	Final diameter of specimen (mm)				46.8
R11-6 Radial	Decrease in diameter mm	Void ratio	*Axial stress* kPa	*Radial stress* kPa	Mean stress kPa	Accumulated swell (%) $\Delta A/A_0 = \Delta V/V_0$	Remarks	Constants $m_{s.start}$ (g) 114
		0.62	0	0			after comp.	ρ_s (kg/m^3)
2009-09-23 10:02	0.0		882	855	864		start	2780
2009-10-27 09:30	0.0	0.68	11,734	11,666	11,688		saturation	e_{calc}
2009-10-27 10:43	6.0		799	476	584			
2009-11-05 15:30	0.0	1.28	997	1,418	1,277	31.3	swell 1	1.44

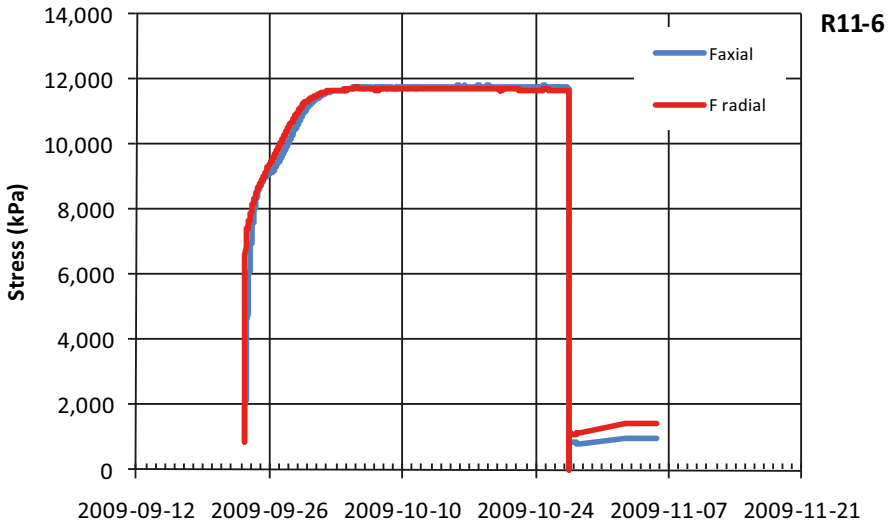

R11-7	Test description:	Total of 2 steps; saturation and 1 steps of swelling (friction minimized)						
R11-7 Axial	Constant height of specimen (mm)		40	Final diameter of specimen (mm)				46.8
R11-7 Radial	Decrease in diameter mm	Void ratio	*Axial stress* kPa	*Radial stress* kPa	Mean stress kPa	Accumulated swell (%) $\Delta A/A_0 = \Delta V/V_0$	Remarks	Constants $m_{s.start}$ (g) 114
		0.62	0	0			after comp.	ρ_s (kg/m^3)
2009-11-20 16:30	0.0		1,411	571	851		start	2,780
2009-11-30 13:30	0.0	0.68	11,478	10,920	11,106		saturation	e_{calc}
2009-11-30 15:35	3.0		891	15	307			
2009-12-07 14:00	0.0	0.97	2,962	3,317	3,199	14.2	swell 1	0.95

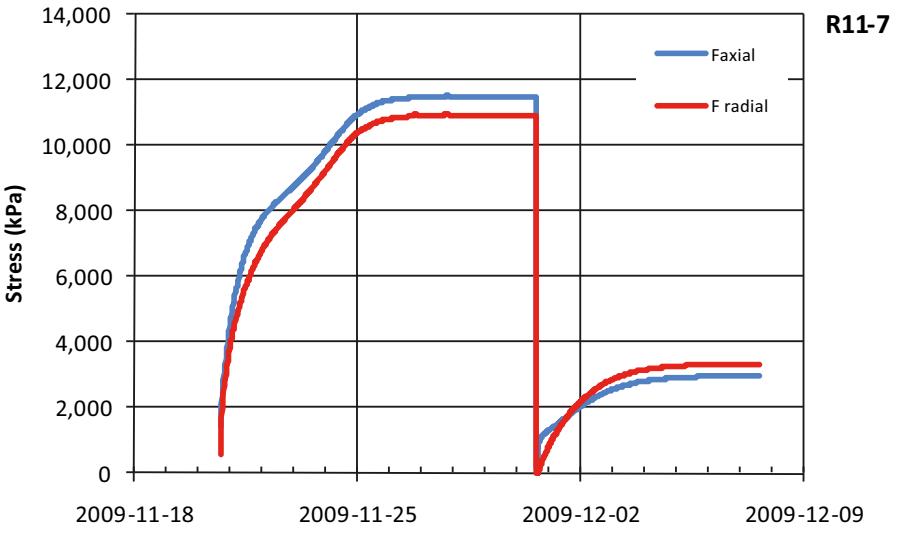

R11-9	Test description:	Total of 2 steps; saturation and 1 steps of swelling (friction minimized)						
R11-9 Axial	Constant height of specimen (mm)		40	Final diameter of specimen (mm)				46.8
R11-9 Radial	Decrease in diameter mm	Void ratio	*Axial stress* kPa	*Radial stress* kPa	Mean stress kPa	Accumulated swell (%) $\Delta A/A_0 = \Delta V/V_0$	Remarks	Constants $m_{s.start}$ (g) 114
		0.62	0	0			after comp.	ρ_s (kg/m^3)
2009-12-17 15:49	0.0		712	599	637		start	2780
2010-01-15 15:00	0.0	0.68	10,269	11,245	10,920		saturation	e_{calc}
2010-01-15 18:00	6.0		958	14	329			
2010-01-22 14:30	0.0	1.25	594	886	789	31.6	swell 1	1.45

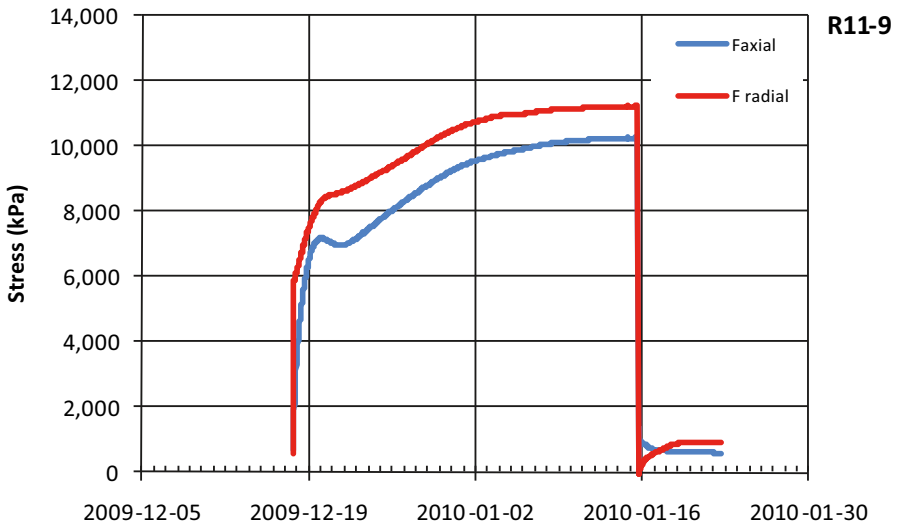

R11-10	Test description:	Total of 2 steps; saturation and 1 steps of swelling (friction minimized)						
R11-10 Axial	Constant height of specimen (mm)	40	Final diameter of specimen (mm)	46.8				
R11-10 Radial	Decrease in diameter mm	Void ratio	*Axial stress* kPa	*Radial stress* kPa	Mean stress kPa	Accumulated swell (%) $\Delta A/A_0 = \Delta V/V_0$	Remarks	Constants $m_{s.start}$ (g) 114
		0.62	0	0			after comp.	ρ_s (kg/m^3)
2009-12-18 14:34	0.0		794	451	565		start	2,780
2009-12-29 13:30	0.0	0.68	10,067	8,950	9,322		saturation	e_{calc}
2009-12-29 14:29	0.7		771	51	291			
2010-01-04 17:00	0.0	0.81	5,798	6,807	6,470	3.0	swell 1	0.73

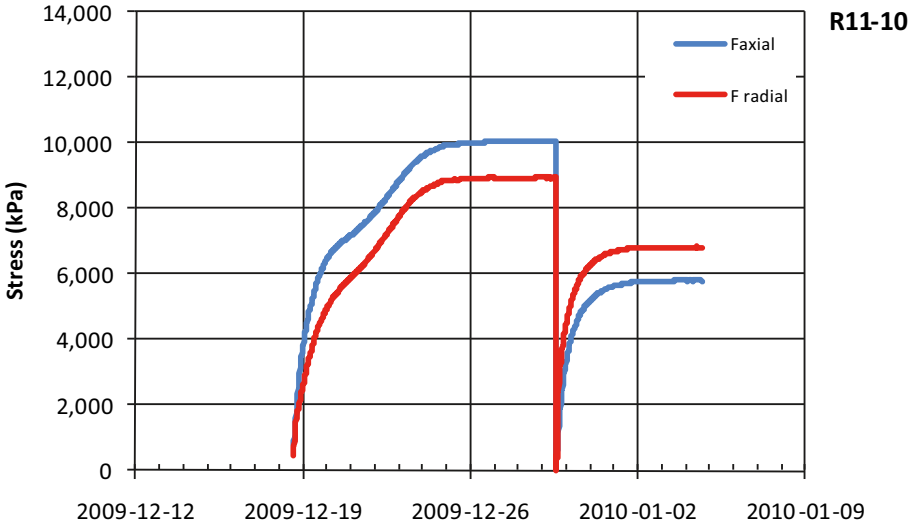

R11-11	**Test description:**	Total of 2 steps; saturation and 1 steps of swelling (friction minimized)						
R11-11 Axial	**Constant height of specimen (mm)**		40	Final diameter of specimen (mm)			46.8	
R11-11 Radial	Decrease in diameter mm	Void ratio	*Axial stress* kPa	*Radial stress* kPa	Mean stress kPa	Accumulated swell (%) $\Delta A/A_0 = \Delta V/V_0$	Remarks	Constants $m_{s.start}$ (g) 114
		0.62	0	0			after comp.	ρ_s (kg/m^3)
2010-01-05 15:06	0.0		745	359	487		start	2,780
2010-01-15 13:30	0.0	0.68	10,066	11,280	10,875		saturation	e_{calc}
2010-01-15 14:33	1.1		645	49	248			
2010-01-21 10:30	0.0	0.84	5,359	5,637	5,544	4.9	swell 1	0.76

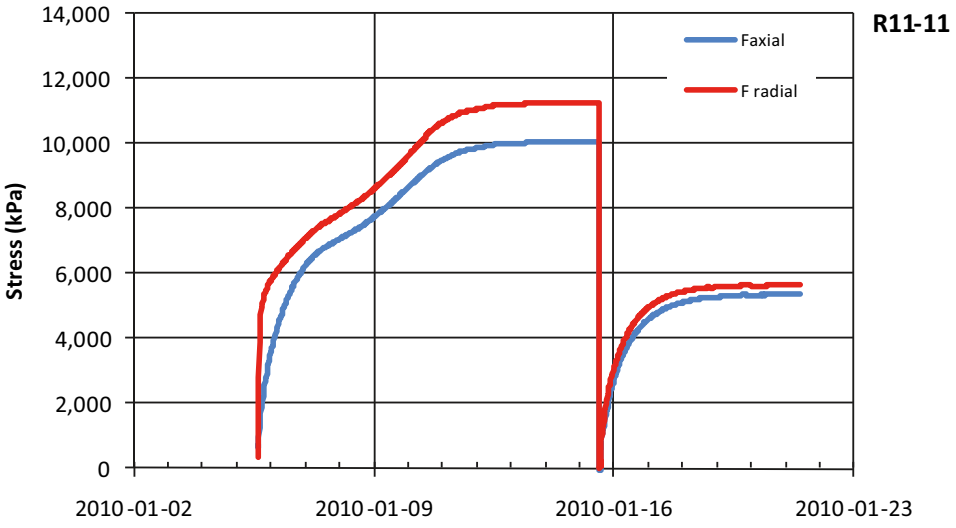

R11-12	Test description:	Total of 2 steps; saturation and 1 steps of swelling (friction minimized)						
R11-12 Axial Iso	Constant height of specimen (mm)		40	Final diameter of specimen (mm)				46.8
R11-12 Radial Iso	Decrease in diameter	Void ratio	*Axial stress*	*Radial stress*	Mean stress	Accumulated swell (%)		Constants $m_{s.start}$ (g)
ISOSTAT	mm		kPa	kPa	kPa	$\Delta A/A_0 = \Delta V/V_0$	Remarks	118.8
		0.45	0	0			drilling	ρ_s (kg/m^3)
2010-03-16 16:45	0.0		853	372	533		start	2,780
2010-03-24 15:00	0.0	0.61	12,635	12,086	12,269		saturation	e_{calc}
2010-03-24 16:45	1.1		796	176	383			
2010-04-06 10:30	0.0	0.72	5,605	5,933	5,824	4.8	swell 1	0.69

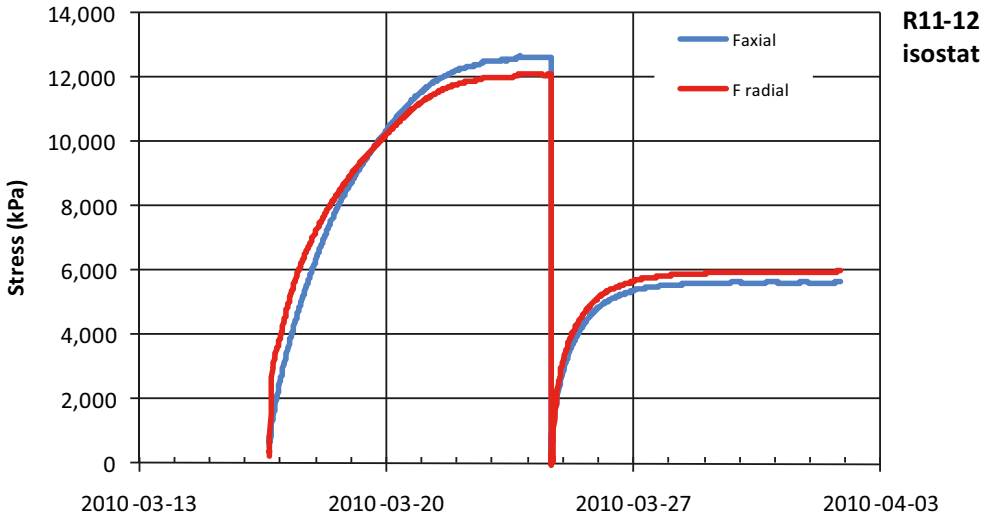

R11-13	Test description:	Total of 2 steps; saturation and 1 steps of swelling (friction minimized)						
R11-13 Axial Iso	Constant height of specimen (mm)		40	Final diameter of specimen (mm)			46.8	
R11-13 Radial Iso	Decrease in diameter mm	Void ratio	*Axial stress* kPa	*Radial stress* kPa	Mean stress kPa	Accumulated swell (%) $\Delta A/A_0 = \Delta V/V_0$	Remarks	Constants $m_{s.start}$ (g) 120.9
ISOSTAT								
		0.45	0	0			drilling*	ρ_s (kg/m^3)
2010-04-09 09:29	0.0		851	483	606		start	2,780
2010-04-28 00:00	0.0	0.58	14,960	17,411	16,594		saturation	e_{calc}
2010-04-29 16:25	5.8		720	0	240			
2010-05-28 02:30	0.0	1.21	1,063	190	481	30.0	swell 1	1.26

* uncertain void ratio

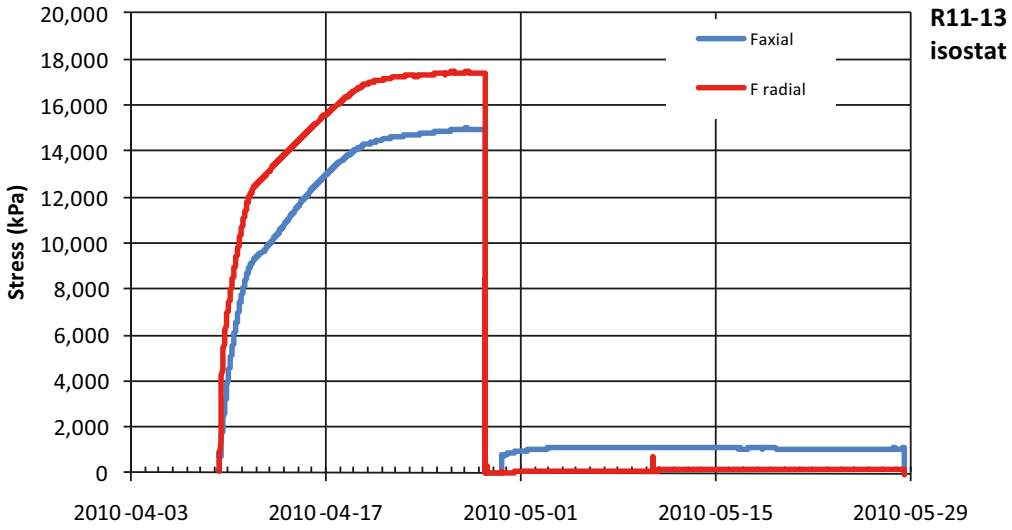

R11-14	Test description:	Total of 2 steps; saturation and 1 steps of swelling (friction minimized).(R11-7)						
R11-14 Axial	Constant height of specimen (mm)		40	Final diameter of specimen (mm)				46.8
R11-14 Radial	Decrease in diameter mm	Void ratio	*Axial stress* kPa	*Radial stress* kPa	Mean stress kPa	Accumulated swell (%) $\Delta A/A_0 = \Delta V/V_0$	Remarks	Constants $m_{s.start}$ (g) 114.0
		0.62	0	0			*	ρ_s (kg/m^3)
2010-06-22 11:05	0.0		668	501	557		start	2,780
2010-07-12 19:30	0.0	0.68	10,719	7,954	8,875		saturation	e_{calc}
2010-07-13 15:53	2.9		661	53	256			
2010-08-15 19:30	0.0	0.97	2,837	2,796	2,809	13.8	swell 1	0.95

* void ratio as in R11-7

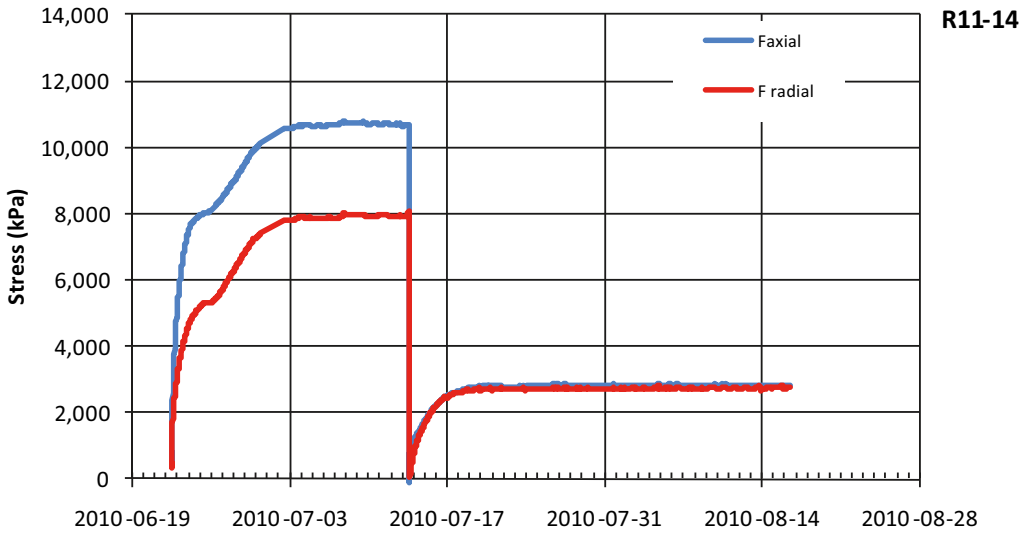

R11-15	Test description:	Total of 2 steps; saturation and 1 steps of swelling (friction min.). Srin=100%						
R11-15 Axial	Constant height of specimen (mm)		40	Final diameter of specimen (mm)				46.8
R11-15 Radial	Decrease in diameter mm	Void ratio	*Axial stress* kPa	*Radial stress* kPa	Mean stress kPa	Accumulated swell (%) $\Delta A/A_0 = \Delta V/V_0$	Remarks	Constants $m_{s.start}$ (g) 113.9
			0	0				ρ_s (kg/m^3)
2010-08-27 09:58	0.0		1,890	1,034	1,320		start	2,780
2010-09-08 11:30	0.0	0.68	10,817	11,536	11,296		saturation	e_{calc}
2010-09-08 15:59	3.0		1,725	29	594			
2010-09-20 10:30	0.0	0.98	3,213	3,671	3,519	14.3	swell 1	0.96

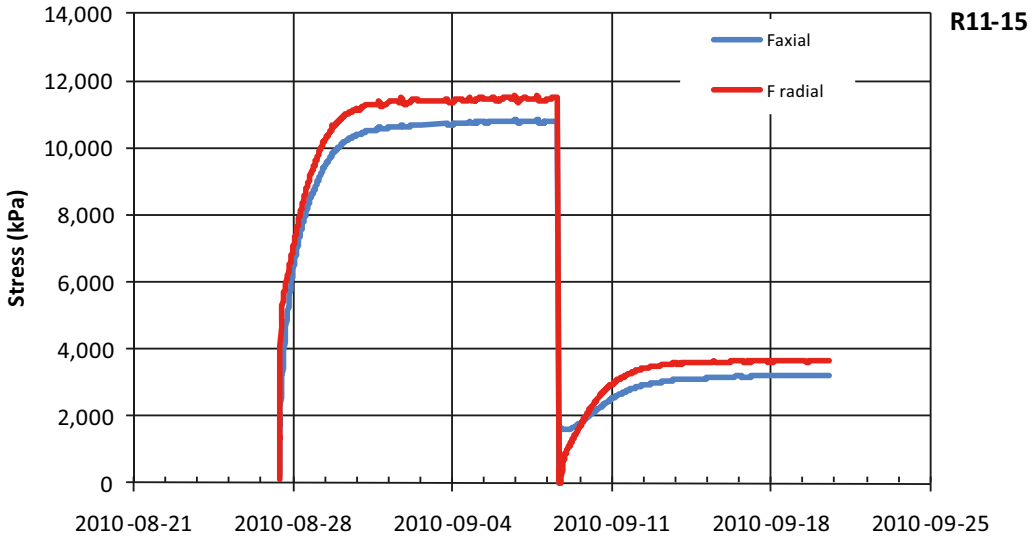

R11-16	**Test description:**	Total of 1 steps; 1 steps of swelling (friction min.). Srini≈100%						
R11-16 Axial	**Constant height of specimen (mm)**		40	Final diameter of specimen (mm)				46.8
R11-16 Radial	Decrease in diameter mm	Void ratio	*Axial stress* kPa	*Radial stress* kPa	Mean stress kPa	Accumulated swell (%) $\Delta A/A_0 = \Delta V/V_0$	Remarks	Constants $m_{s.swell}$ (g) 100.3
								ρ_s (kg/m^3)
	0.0							2,780
	0.0	0.68					start	e_{calc}
2010-10-12 12:00	3.4		1,760	9	593			
2010-10-25 08:30	0.0	0.93	3,675	3,473	3,540	16.3	swell 1	0.91

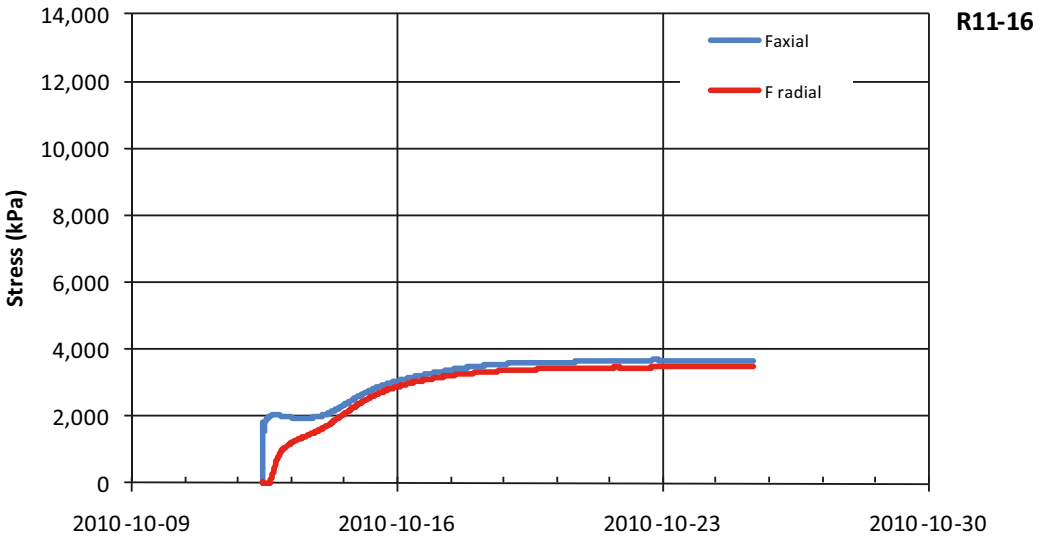

A1-3 Radial swelling into cavity

R21-3	**Test description:**	Total of 2 steps; saturation and 1 steps of swelling (friction minimized)						
R21-3 Axial	**Constant height of specimen (mm)**		40	Final diameter of specimen (mm)				46.8
R21-3 Radial	Diameter of cavity mm	Void ratio	*Axial stress* kPa	*Radial stress* kPa	Mean stress kPa	Accumulated swell (%) $\Delta A/A_0=\Delta V/V_0$	Remarks	Constants $m_{s.start}$ (g) 114
	0.0	0.62	0	0			after comp	ρ_s (kg/m^3)
2009-03-18 13:44	0.0		1,152	684	840		start	2,780
2009-03-26 14:18	0.0	0.68	13,112	14,109	13,777		saturation	e_{calc}
2009-03-26 14:37	8.0		850	6,056	4,321			
2009-04-06 14:00	0.0	0.80	6,849	7,604	7,352	3.0	swell 1	0.73

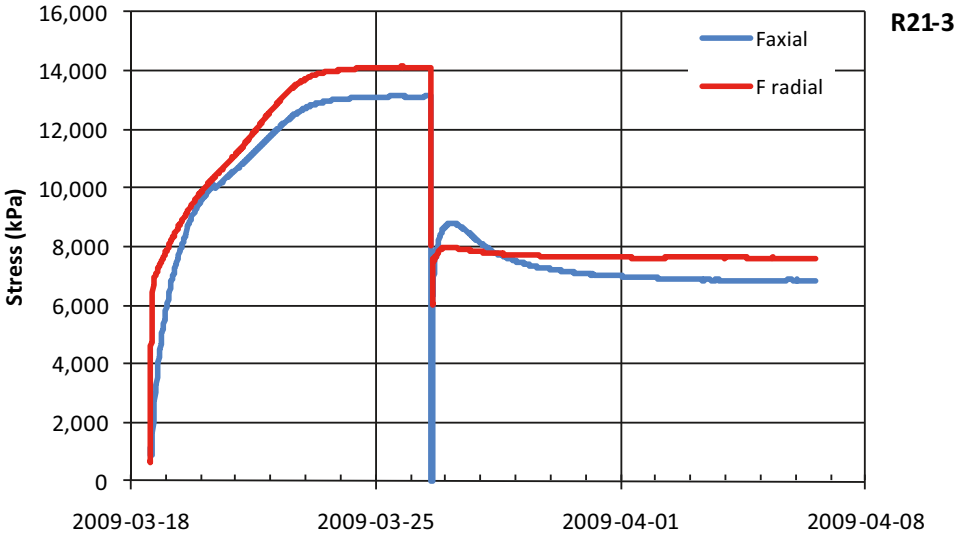

R21-5	**Test description:**	Total of 2 steps; saturation and 1 steps of swelling (friction minimized)						
R21-5 Axial	**Constant height of specimen (mm)**	40		Final diameter of specimen (mm)				46.8
R21-5 Radial	Diameter of cavity mm	Void ratio	*Axial stress* kPa	*Radial stress* kPa	Mean stress kPa	Accumulated swell (%) $\Delta A/A_0=\Delta V/V_0$	Remarks	Constants $m_{s.start}$ (g) 114
	0.0	0.62	0	0			after comp	ρ_s (kg/m^3)
2009-06-24 16:22	0.0		873	748	790		start	2,780
2009-07-06 13:00	0.0	0.68	11,329	13,063	12,485		saturation	e_{calc}
2009-07-06 14:01	10.5		5,693	6,624	6,314			
2009-07-14 09:00	0.0	0.83	5,523	6,711	6,315	5.3	swell 1	0.77

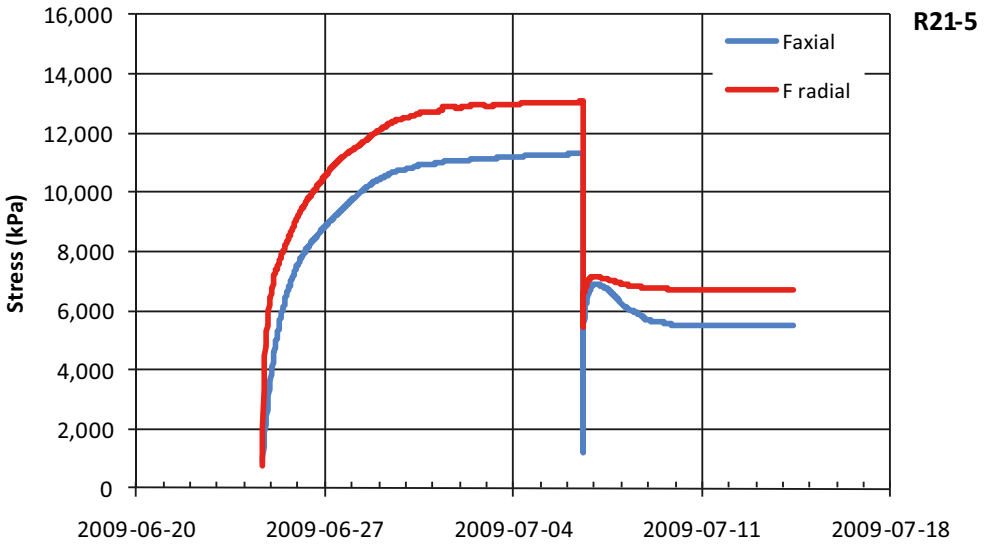

R21-6	**Test description:**	Total of 2 steps; saturation and 1 steps of swelling (friction minimized)						
R21-6 Axial	**Constant height of specimen (mm)**		40	Final diameter of specimen (mm)				46.8
R21-6 Radial	Diameter of cavity mm	Void ratio	*Axial stress* kPa	*Radial stress* kPa	Mean stress kPa	Accumulated swell (%) $\Delta A/A_0=\Delta V/V_0$	Remarks	Constants $m_{s.start}$ (g) 114
	0.0	0.62	0	0			after comp	ρ_s (kg/m^3)
2009-07-15 11:31	0.0		1,126	422	657		start	2,780
2009-08-04 10:00	0.0	0.68	9,961	10,401	10,254		saturation	e_{calc}
2009-08-04 11:05	19.0		4,352	3,514	3,793			
2009-08-12 13:30	0.0	1.13	2,244	1,401	1,682	19.7	swell 1	1.09

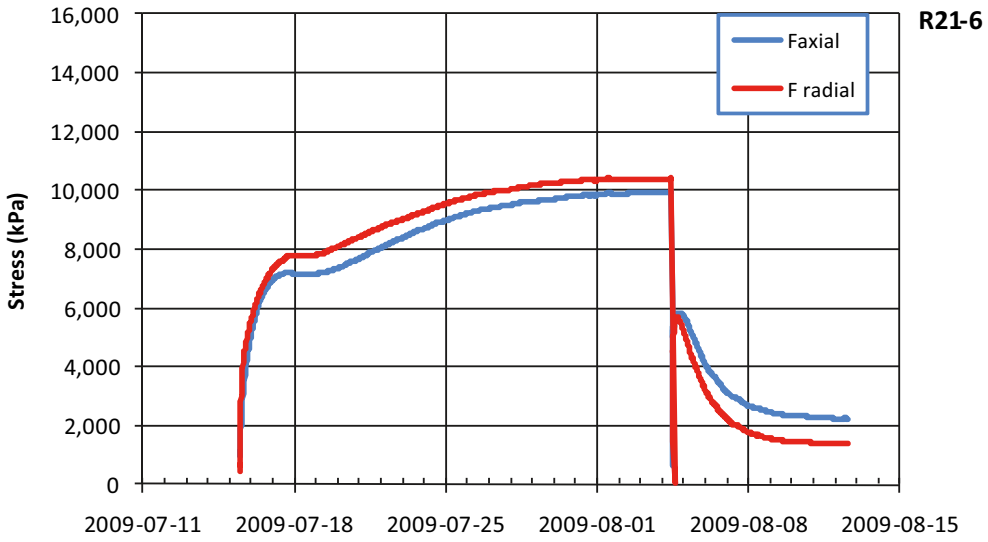

R21-7	Test description:	Total of 1 steps; saturation						
R21-7 Axial	Constant height of specimen (mm)		40	Final diameter of specimen (mm)				46.8
R21-7 Radial	Diameter of cavity mm	Void ratio	*Axial stress* kPa	*Radial stress* kPa	Mean stress kPa	Accumulated swell (%) $\Delta A/A_0=\Delta V/V_0$	Remarks	Constants $m_{s.start}$ (g) 114
	0.0	0.62	0	0			after comp	ρ_s (kg/m^3)
2009-08-13 15:09	0.0		676	774	741		start	2,780
2009-08-31 10:30	0.0	0.72	12,086	6,694	8,491		saturation	e_{calc} 0.68

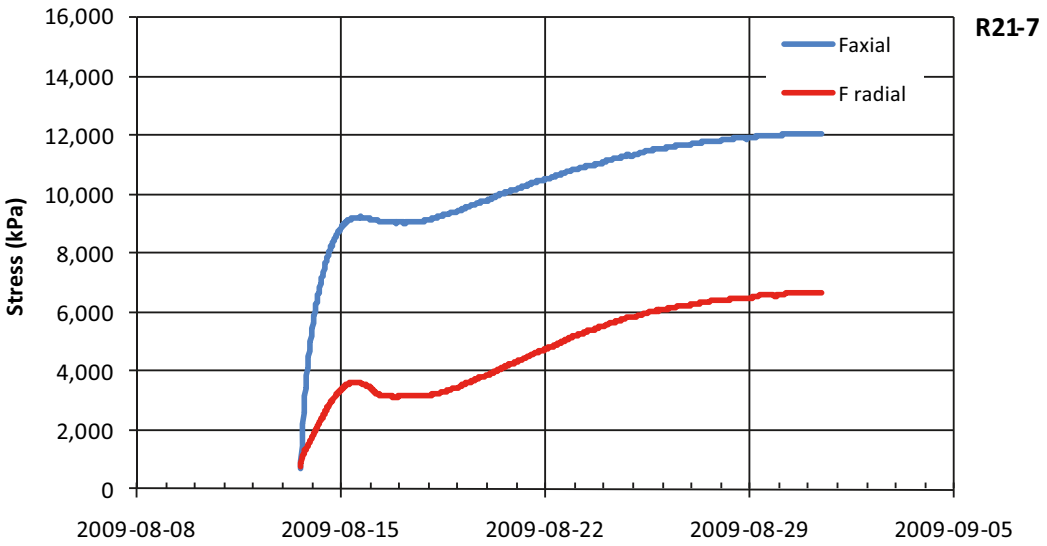

R21-8	**Test description:**	Total of 2 steps; saturation and 1 steps of swelling (friction minimized)						
R21-8 Axial	**Constant height of specimen (mm)**		40	Final diameter of specimen (mm)				46.8
R21-8 Radial	Diameter of cavity mm	Void ratio	*Axial stress* kPa	*Radial stress* kPa	Mean stress kPa	Accumulated swell (%) $\Delta A/A_0=\Delta V/V_0$	Remarks	Constants $m_{s.start}$ (g) 114
	0.0	0.62	0	0			after comp	ρ_s (kg/m^3)
2009-09-01 14:18	0.0		1,070	883	945		start	2,780
2009-09-21 09:00	0.0	0.68	13,173	13,106	13,129		saturation	e_{calc}
2009-09-21 17:00	23.0		2,536	2,022	2,193			
2009-10-22 11:30	0.0	1.22	1,196	667	843	31.8	swell 1	1.46

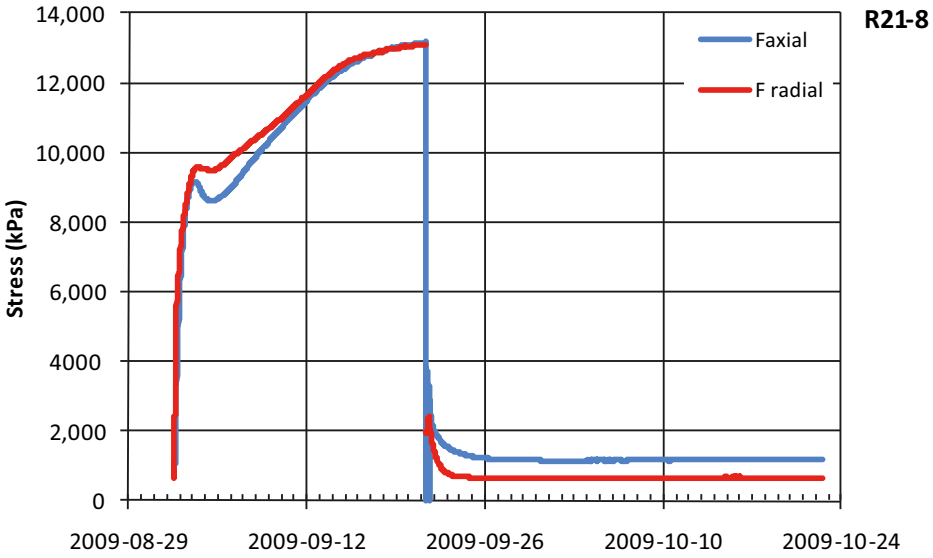

Appendix 2

Distribution of basic variables over the specimen height (tables)

The distribution of the basic variables water content w, bulk density ρ, void ratio, dry density ρ_d and degree of saturation S_r, over the specimen height are given for all tests. Each series is presented in separate appendices.

A2-1 Axial swelling

A01-1

from bottom mm	thickness mm	ρ_s kg/m³	ρ_w kg/m³	w %	ρ kg/m³	e	ρ_d kg/m³	S_r %
3.55	7.1	2,780	1,000	38.1	1,861	1.06	1,347	100
10.78	7.36	2,780	1,000	37.7	1,870	1.05	1,358	100
18.81	8.7	2,780	1,000	41.2	1,827	1.15	1,294	100
	average			39.0	1,852	1.09	1,333	100

A01-2

from bottom mm	thickness mm	ρ_s kg/m³	ρ_w kg/m³	w %	ρ kg/m³	e	ρ_d kg/m³	S_r %
3.805	7.61	2,780	1,000	38.2	1,852	1.07	1,340	99
11.39	7.56	2,780	1,000	37.6	1,862	1.05	1,354	99
19.37	8.4	2,780	1,000	41.1	1,822	1.15	1,291	99
	average			39.0	1,845	1.09	1,328	99

A01-3

from bottom mm	thickness mm	ρ_s kg/m³	ρ_w kg/m³	w %	ρ kg/m³	e	ρ_d kg/m³	S_r %
3.75	7.5	2,780	1,000	37.6	1,855	1.06	1,348	98
11	7	2,780	1,000	38.5	1,850	1.08	1,336	99
18	7	2,780	1,000	41.7	1,823	1.16	1,286	100
	average			39.3	1,843	1.10	1,323	99

A01-5

from bottom mm	thickness mm	ρ_s kg/m³	ρ_w kg/m³	w %	ρ kg/m³	e	ρ_d kg/m³	S_r %
	6	2,780	1,000	44.1	1,780	1.25	1,235	98
	6	2,780	1,000	37.6	1,843	1.08	1,339	97
	6	2,780	1,000	38.9	1,860	1.08	1,339	100
	6	2,780	1,000	36.2	1,866	1.03	1,370	98
	average			39.2	1,837	1.11	1,320	98

A01-7

from bottom mm	thickness mm	ρ_s kg/m³	ρ_w kg/m³	w %	ρ kg/m³	e	ρ_d kg/m³	S_r %
0	average			25.1	2,016	0.72	1,612	96
25	average			25.1	2,016	0.72	1,612	96
	average			25.1	2,016	0.72	1,612	96

A01-8

from bottom	thickness	ρ_s	ρ_w	w	ρ	e	ρ_d	S_r
mm	mm	kg/m^3	kg/m^3	%	kg/m^3		kg/m^3	%
5	10	2,780	1,000	36.7	1,864	1.04	1,364	98
13.5	7	2,780	1,000	38.5	1,844	1.09	1,332	98
20.5	7	2,780	1,000	46.3	1,777	1.29	1,214	100
	average			40.5	1,828	1.14	1,301	99

A01-9

from bottom	thickness	ρ_s	ρ_w	w	ρ	e	ρ_d	S_r
mm	mm	kg/m^3	kg/m^3	%	kg/m^3		kg/m^3	%
5	10	2,780	1,000	35.8	1,883	1.01	1,386	99
13.5	7	2,780	1,000	37.7	1,857	1.06	1,349	99
19.5	5	2,780	1,000	41.6	1,801	1.19	1,272	98
23.5	3	2,780	1,000	48.8	1,740	1.38	1,170	99
	average			39.0	1,842	1.10	1,325	99

A01-10

from bottom	thickness	ρ_s	ρ_w	w	ρ	e	ρ_d	S_r
mm	mm	kg/m^3	kg/m^3	%	kg/m^3		kg/m^3	%
6	12	2,780	1,000	41.0	1,823	1.15	1,293	99
16	8	2,780	1,000	43.4	1,797	1.22	1,253	99
22.5	5	2,780	1,000	50.6	1,723	1.43	1,144	98
26.5	3	2,780	1,000	63.1	1,642	1.76	1,007	100
	average			45.8	1,778	1.29	1,220	99

A2-2 Radial swelling of the outer surface

R11-1

radius mm	thickness mm	ρ_s kg/m³	ρ_w kg/m³	w %	ρ kg/m³	e	ρ_d kg/m³	Sr %
5	10	2,780	1,000	34.4	1,890	0.98	1,407	98
	8.4	2,780	1,000	25.4	2,010	0.72	1,603	98
20.9	5	2,780	1,000	36.3	1,888	1.01	1,385	100
	average			31.2	1,941	0.88	1,480	99

R11-2

radius mm	thickness mm	ρ_s kg/m³	ρ_w kg/m³	w %	ρ kg/m³	e	ρ_d kg/m³	Sr %
5	10	2,780	1,000	25.7	2,024	0.73	1,611	98
	8.4	2,780	1,000	25.9	2,011	0.74	1,598	97
20.9	5	2,780	1,000	28.9	1,967	0.82	1,526	98
	average			27.0	1,997	0.77	1,572	98

R11-5

radius mm	thickness mm	ρ_s kg/m³	ρ_w kg/m³	w %	ρ kg/m³	e	ρ_d kg/m³	Sr %
5	10	2,780	1,000	26.8	2,008	0.76	1,583	99
	8.4	2,780	1,000	28.5	1,981	0.80	1,541	99
20.9	5	2,780	1,000	30.3	1,949	0.86	1,496	98
	average			28.9	1,974	0.82	1,531	98

R11-6

radius mm	thickness mm	ρ_s kg/m³	ρ_w kg/m³	w %	ρ kg/m³	e	ρ_d kg/m³	Sr %
5	10	2,780	1,000	40.8	1,816	1.16	1,290	98
	8.4	2,780	1,000	44.5	1,833	1.18	1,269	104
20.9	5	2,780	1,000	51.3	1,725	1.44	1,140	99
	average			46.4	1,789	1.28	1,221	101

R11-7

radius mm	thickness mm	ρ_s kg/m³	ρ_w kg/m³	w %	ρ kg/m³	e	ρ_d kg/m³	Sr %
5	10	2,780	1,000	31.7	1,930	0.90	1,466	98
	8.4	2,780	1,000	33.9	1,930	0.93	1,441	102
20.9	5	2,780	1,000	37.0	1,858	1.05	1,356	98
	average			34.7	1,903	0.97	1,413	100

R11-9

radius mm	thickness mm	ρ_s kg/m³	ρ_w kg/m³	w %	ρ kg/m³	e	ρ_d kg/m³	Sr %
5	10	2,780	1,000	35.4	1,847	1.04	1,364	95
	8.4	2,780	1,000	43.8	1,714	1.33	1,192	92
20.9	5	2,780	1,000	43.1	1,760	1.26	1,230	95
	average			42.0	1,756	1.25	1,236	94

R11-10

radius mm	thickness mm	ρ_s kg/m^3	ρ_w kg/m^3	w %	ρ kg/m^3	e	ρ_d kg/m^3	Sr %
5	10	2,780	1,000	26.5	2,018	0.74	1,595	99
	8.4	2,780	1,000	29.6	1,978	0.82	1,527	100
20.9	5	2,780	1,000	29.9	1,967	0.84	1,514	99
	average			29.1	1,981	0.81	1,534	100

R11-11

radius mm	thickness mm	ρ_s kg/m^3	ρ_w kg/m^3	w %	ρ kg/m^3	e	ρ_d kg/m^3	Sr %
5	10	2,780	1,000	27.0	2,008	0.76	1,581	99
	8.4	2,780	1,000	31.6	1,959	0.87	1,489	102
20.9	5	2,780	1,000	30.3	1,954	0.85	1,500	99
	average			30.3	1,966	0.84	1,510	100

R11-12

radius mm	thickness mm	ρ_s kg/m^3	ρ_w kg/m^3	w %	ρ kg/m^3	e	ρ_d kg/m^3	Sr %
4	8	2,780	1,000	24.4	2,047	0.69	1,646	98.3
12	8	2,780	1,000	24.8	2,045	0.70	1,639	99.0
20	8	2,780	1,000	27.6	2,003	0.77	1,570	99.5
	average			26.3	2,022	0.74	1,601	99.2

R11-13

radius mm	thickness mm	ρ_s kg/m^3	ρ_w kg/m^3	w %	ρ kg/m^3	e	ρ_d kg/m^3	Sr %
4	8	2,780	1,000	38.5	1,859	1.07	1,342	99.9
12	8	2,780	1,000	40.3	1,828	1.13	1,302	98.8
20	8	2,780	1,000	45.7	1,776	1.28	1,219	99.1
	average			43.1	1,803	1.21	1,260	99.1

R11-14

radius mm	thickness mm	ρ_s kg/m^3	ρ_w kg/m^3	w %	ρ kg/m^3	e	ρ_d kg/m^3	Sr %
4	8	2,780	1,000	34.6	1,922	0.95	1,428	101.6
12	8	2,780	1,000	34.1	1,900	0.96	1,417	98.5
20	8	2,780	1,000	34.9	1,891	0.98	1,402	98.7
	average			34.6	1,898	0.97	1,410	99.0

R11-15

radius mm	thickness mm	ρ_s kg/m^3	ρ_w kg/m^3	w %	ρ kg/m^3	e	ρ_d kg/m^3	Sr %
4	8	2,780	1,000	31.6	1,934	0.89	1,470	98.5
12	8	2,780	1,000	32.8	1,918	0.93	1,444	98.6
20	8	2,780	1,000	36.6	1,877	1.02	1,374	99.3
	average			34.8	1,897	0.98	1,407	99.0

R11-16

radius mm	thickness mm	ρ_s kg/m³	ρ_w kg/m³	w %	ρ kg/m³	e	ρ_d kg/m³	Sr %
4	8	2,780	1,000	30.6	1,961	0.85	1,502	99.8
12	8	2,780	1,000	31.3	1,948	0.87	1,483	99.6
20	8	2,780	1,000	35.0	1,896	0.98	1,404	99.4
	average			33.3	1,921	0.93	1,441	99.5

A2-3 Radial swelling into cavity

R21-3

radius mm	thickness mm	ρ_s kg/m³	ρ_w kg/m³	w %	ρ kg/m³	e	ρ_d kg/m³	Sr %
5	10	2,780	1,000	31.3	1,939	0.88	1,477	99
	8.4	2,780	1,000	28.0	2,003	0.78	1,565	100
20.9	5	2,780	1,000	26.9	1,984	0.78	1,563	96
	average			28.2	1,984	0.80	1,548	98

R21-5

radius mm	thickness mm	ρ_s kg/m³	ρ_w kg/m³	w %	ρ kg/m³	e	ρ_d kg/m³	Sr %
5	10	2,780	1,000	32.4	1,900	0.94	1,435	96
	8.4	2,780	1,000	28.5	1,944	0.84	1,513	95
20.9	5	2,780	1,000	27.0	1,988	0.78	1,565	97
	average			28.6	1,953	0.83	1,518	96

R21-6

radius mm	thickness mm	ρ_s kg/m³	ρ_w kg/m³	w %	ρ kg/m³	e	ρ_d kg/m³	Sr %
5	10	2,780	1,000	47.0	1,737	1.35	1,181	97
	8.4	2,780	1,000	41.9	1,869	1.10	1,317	105
20.9	5	2,780	1,000	37.1	1,856	1.05	1,354	98
	average			41.0	1,840	1.13	1,305	101

R21-7

radius mm	thickness mm	ρ_s kg/m³	ρ_w kg/m³	w %	ρ kg/m³	e	ρ_d kg/m³	Sr %
5	10	2,780	1,000	23.3	2,047	0.67	1,660	96
	8.4	2,780	1,000	24.2	1,997	0.73	1,607	92
20.9	5	2,780	1,000	25.1	2,011	0.73	1,608	96
	average			24.4	2,011	0.72	1,617	94

R21-8

radius mm	thickness mm	ρ_s kg/m³	ρ_w kg/m³	w %	ρ kg/m³	e	ρ_d kg/m³	Sr %
5	10	2,780	1,000	48.7	1,734	1.38	1,166	98
	8.4	2,780	1,000	40.6	1,730	1.25	1,230	90
20.9	5	2,780	1,000	37.8	1,820	1.10	1,321	95
	average			41.0	1,765	1.22	1,252	93

Appendix 3

Final results of basic variables and swelling pressure (tables)

In the tables the final values of the basic variables (water content w, bulk density ρ, dry density ρ_d, degree of saturation S_r) and the swelling pressure (axial P_a, radial P_r) are given. The last column contains the total time for each test divided into the time for saturation t_1 and the time for homogenisation t_2 ($t_1 + t_2$).

Table A3-1. Results from series A01.

Sample ID	Swelling (%)	Average over specimen height w (%)	ρ (kg/m³)	ρ_d (kg/m³)	S_r (%)	Swelling pressure Axial P_a (kPa)	Radial P_r (kPa)	Total time (days)
A01-1	25	39.0	1,852	1,333	100	1,137	1,819	25 + 70
A01-2	26	39.0	1,845	1,328	99	1,065	1,826	9 + 18
A01-3	26	39.3	1,843	1,323	99	1,016	1,414	11 + 49
A01-5	26	39.2	1,837	1,320	98	1,363	1,645	0 + 27
A01-7	0	25.1	2,016	1,612	96	9,548	10,045	12 + 0
A01-8	25	40.5	1,828	1,301	99	1,363	1,645	23 + 0
A01-9	26	39.0	1,842	1,325	99	1,333	1,716	16 + 11
A01-10	38	45.8	1,778	1,220	99	771	775	18 + 22

Table A3-2. Results from series R11.

Sample ID	Swelling (%)	Average over specimen height w (%)	ρ (kg/m³)	ρ_d (kg/m³)	S_r (%)	Swelling pressure Axial P_a (kPa)	Radial P_r (kPa)	Total time[1] (days)
R11-1	14	31.2	1,941	1,480	99	3,162	4,111	8 + 6
R11-2	3	27.0	1,997	1,572	98		7,530	8 + 15
R11-5	5	28.9	1,974	1,531	98	6,279	7,936	6 + 5
R11-6	31	46.4	1,789	1,221	101	997	1,418	34 + 9
R11-7	14	34.7	1,903	1,413	100	2,962	3,317	10 + 7
R11-9	32	42.0	1,756	1,236	94	594	886	29 + 7
R11-10	3	29.1	1,981	1,534	100	5,798	6,807	11 + 6
R11-11	5	30.3	1,966	1,510	100	5,359	5,637	10 + 6
R11-12	5	26.3	2,022	1,601	99	5,605	5,933	8 + 13
R11-13	30	43.1	1,803	1,260	99	1,063	190	19 + 30
R11-14	14	34.6	1,898	1,410	99	2,837	2,796	20 + 34
R11-15	14	34.8	1,897	1,407	99	3,213	3,671	12 + 12
R11-16	16	33.3	1,921	1,441	100	3,675	3,473	0 + 13

Table A3-3. Results from series R21.

Sample ID	Swelling (%)	Average over specimen height w (%)	ρ (kg/m³)	ρ_d (kg/m³)	S_r (%)	Swelling pressure Axial P_a (kPa)	Radial P_r (kPa)	Total time (days)
R21-3	3	28.2	1,984	1,548	98	6,849	7,604	8 + 11
R21-5	5	28.6	1,953	1,518	96	5,523	6,711	12 + 8
R21-6	20	41.0	1,840	1,305	101	2,244	1,401	20 + 8
R21-7	0	24.4	2,011	1,617	94	12,086	6,694	18 + 0
R21-8	32	41.0	1,765	1,252	93	1,196	667	20 + 31